Molecular Biology of the Cell
Vol. 17, 2824–2838, June 2006

Cdc42p GDP/GTP Cycling Is Necessary for Efficient Cell Fusion during Yeast Mating

Sophie Barale,*† Derek McCusker,†‡ and Robert A. Arkowitz*

*Institute of Signaling, Developmental Biology, and Cancer, Centre National de la Recherche Scientifique UMR 6543, Université de Nice, Faculté des Sciences-Parc Valrose, 06108 Nice Cedex 2, France; and ‡Department of Biology, Sinsheimer Laboratories, University of California at Santa Cruz, Santa Cruz, CA 95064

Submitted November 14, 2005; Revised March 2, 2006; Accepted March 20, 2006
Monitoring Editor: Janet Shaw

The highly conserved small Rho G-protein, Cdc42p plays a critical role in cell polarity and cytoskeleton organization in all eukaryotes. In the yeast *Saccharomyces cerevisiae*, Cdc42p is important for cell polarity establishment, septin ring assembly, and pheromone-dependent MAP-kinase signaling during the yeast mating process. In this study, we further investigated the role of Cdc42p in the mating process by screening for specific mating defective *cdc42* alleles. We have identified and characterized novel mating defective *cdc42* alleles that are unaffected in vegetative cell polarity. Replacement of the Cdc42p Val36 residue with Met resulted in a specific cell fusion defect. This *cdc42*[*V36M*] mutant responded to mating pheromone but was defective in cell fusion and in localization of the cell fusion protein Fus1p, similar to a previously isolated *cdc24* (*cdc24-m6*) mutant. Overexpression of a fast cycling Cdc42p mutant suppressed the *cdc24-m6* fusion defect and conversely, overexpression of Cdc24p suppressed the *cdc42*[*V36M*] fusion defect. Taken together, our results indicate that Cdc42p GDP–GTP cycling is critical for efficient cell fusion.

INTRODUCTION

Eukaryotic cells respond to a range of different external signals by gene induction, protein recruitment and activation, and morphological changes. Such responses are critical during diverse developmental processes. The mating process in the yeast *Saccharomyces cerevisiae* is an ideal system for investigating external signal-mediated responses as exposure to mating pheromone triggers an ordered series of events, which terminates in the formation of a diploid zygote. During mating in *S. cerevisiae*, *MAT***a** and *MAT*α cells respond to peptide pheromones, α- and **a**-factor, respectively, secreted by cells of the opposite mating type (for reviews see Sprague and Thorner, 1992; Leberer *et al.*, 1997; Dohlman and Thorner, 2001). These mating pheromones bind to specific G-protein–coupled receptors on each cell type and receptor activation results in cell cycle arrest, transcriptional induction of mating-specific genes, morphological changes leading to formation of a pear-shaped shmoo, and polarized growth toward a mating partner. In response to pheromone, the actin cytoskeleton and secretory apparatus polarize toward the tip of the mating projection (Baba *et al.*, 1989; Read *et al.*, 1992; Smith *et al.*, 2001), and new cell wall and plasma membrane material is deposited at this unique location, which becomes the site of cell contact and ultimately fusion (Lipke *et al.*, 1976; Tkacz and MacKay, 1979). In particular, polarized growth is necessary for positioning the cell fusion apparatus to the site of cell contact. During mating, two yeast cells physically attach to one another forming a prezygote with a continuous extracellular matrix. Specific degradation of the cell wall material at the prezygote septum is necessary so that the plasma membranes can become tightly apposed and fuse. Subsequently, nuclear migration and nuclear fusion result in the formation of a diploid zygote.

The binding of pheromone to the G-protein–coupled pheromone receptor results in release of the $\beta\gamma$ subunits of the heterotrimeric G-protein. This heterodimer G$\beta\gamma$ is critical for activation of the mitogen-activated protein kinase (MAPK) cascade that is necessary for G_1 cell cycle arrest and mating-specific gene transcription. In addition, released G$\beta\gamma$ is required for cell shape changes and oriented growth along a pheromone gradient (chemotropism) via interactions with the guanine nucleotide exchange factor Cdc24p and the cyclin-dependent kinase inhibitor Far1p (Valtz *et al.*, 1995; Butty *et al.*, 1998; Nern and Arkowitz, 1998, 1999). Recently, it has been shown that the released Gα subunit can bind the MAP kinase Fus3p, which subsequently phorphorylates the formin Bni1p (Metodiev *et al.*, 2002; Matheos *et al.*, 2004), both of which are necessary for cell fusion leading to a diploid zygote (Dorer *et al.*, 1997).

Proteins involved in different signaling processes, such as osmotic balance (Philips and Herskowitz, 1997; Nelson *et al.*, 2004), cell wall remodeling (Santos *et al.*, 1997; Fitch *et al.*, 2004), cell polarization (Valtz and Herskowitz, 1996; Dorer *et al.*, 1997; Gammie *et al.*, 1998), and pheromone response (Brizzio *et al.*, 1996; Elia and Marsh, 1998) are important for cell fusion. In addition, several proteins that are highly induced by mating pheromone including the integral membrane protein Fus1p and the cytoplasmic protein Fus2p, which binds the yeast amphiphysin ortholog Rvs161p (Brizzio *et al.*, 1998), are thought to have a specific function in cell fusion (Trueheart *et al.*, 1987) and interact with a range of proteins implicated in

This article was published online ahead of print in *MBC in Press* (http://www.molbiolcell.org/cgi/doi/10.1091/mbc.E05–11–1040) on March 29, 2006.

† These authors contributed equally to this work.

Address correspondence to: Robert A. Arkowitz (arkowitz@unice.fr).

cell fusion (Nelson *et al.*, 2004). These proteins may serve as a scaffold or platform for proteins involved in pheromone signaling and polarity. Fus1p and Fus2p localize to the region of cell fusion before cell wall degradation (Trueheart *et al.*, 1987; Elion *et al.*, 1995; Brizzio *et al.*, 1998), where clusters of vesicles have been observed by electron microscopy (Gammie *et al.*, 1998). *Fus1* mutants do not accumulate such vesicles at the zone of cell fusion, whereas *fus2* mutants accumulate vesicles at this region (Gammie *et al.*, 1998). For plasma membrane fusion the integral membrane protein, Prm1p is important for stabilizing membrane fusion after septum degradation (Heiman and Walter, 2000; Jin *et al.*, 2004).

The highly conserved small GTPase Cdc42p and its guanine nucleotide exchange factor Cdc24p are critical for polarized growth during budding (Johnson, 1999). Cdc42p has been shown to also be required for pseudohyphal and invasive filamentous growth (Mosch *et al.*, 2001). Temperature-sensitive *cdc42* and *cdc24* mutants are defective in pheromone-dependent *FUS1* induction and G_1 arrest at the nonpermissive temperature (Simon *et al.*, 1995); however, these effects are likely to be due to an unresponsiveness to pheromone as a result of cells in an inappropriate cell cycle stage (Oehlen and Cross, 1998). Several α-factor resistant alleles of *cdc42* have been isolated that are defective in PAK kinase interactions indicating that this G-protein functions in pheromone-dependent MAP-kinase signaling (Moskow *et al.*, 2000). Mating-specific *cdc24* mutants have been isolated that are chemotropism defective (Nern and Arkowitz, 1998), and more recently, *cdc24* alleles that are defective in cell fusion have been isolated (Barale *et al.*, 2004). These *cdc24* alleles defective in cell fusion during mating have mutations in conserved residues of the catalytic exchange factor domain, raising the possibility that Cdc42p might also be important for cell fusion. The role of this GTPase module could be analogous to that of the guanine nucleotide exchange factor Myoblast city (a DOCK-180 homolog) and the small G-protein Rac1 during *Drosophila* myoblast fusion (Nolan *et al.*, 1998; Hakeda-Suzuki *et al.*, 2002). Consistent with this hypothesis, a recent study examining two-hybrid interactions of Fus1p showed that a GTP-locked Cdc42p mutant (G12V) interacts with Fus1p and Fus2p (Nelson *et al.*, 2004).

In this study, we show that the highly conserved Rho G-protein Cdc42p is necessary for cell fusion in yeast. We identified mating-specific *cdc42* mutants that had a valine-to-methionine change in position 36 in the Switch I region. This *cdc42* mutant responds to mating pheromone but is defective in cell fusion and in localizing Fus1p to the site of polarized growth, similar to the previously isolated *cdc24-m6* mutant. Overexpression of a fast cycling Cdc42p mutant suppresses the *cdc24-m6* fusion defect, and conversely, overexpression of Cdc24p suppresses the *cdc42[V36M]* fusion defect. Together our results indicate that Cdc42p GDP–GTP cycling is critical for cell fusion.

MATERIALS AND METHODS

General Techniques

Standard techniques and media were used for yeast growth and genetic manipulation (Rose *et al.*, 1991), and unless otherwise indicated yeast were grown at 30°C.

Strains and Plasmids

The strains used in this study are described in Table 1. *CDC42* deletion strains were generated either with a knockout cassette (Δ1) or by polymerase chain reaction (PCR)-mediated gene replacement (Δ2; Nern and Arkowitz, 1999). The knockout cassette was constructed from pBSCDC42 (*CDC42* ORF with 147 nucleotides 3′ of stop codon) with *LEU2* replacing all but the first 62 and the last 15 codons. *STE18* deletion strain was generated by PCR-mediated gene replacement (Nern and Arkowitz, 1999). Gene disruptions were confirmed by PCR and phenotype. A *cdc24*Δ *cdc42*Δ haploid strain with *CDC24* and *CDC42* on CEN plasmids (RAY1728) was obtained by crossing the corresponding single deletion strains (a derivative of RAY1052 with a pRS414CDC24 and RAY1556) followed by sporulation. *Cdc24 cdc42* double mutant strains were generated by transformation and plasmid shuffling of RAY1728. For all experiments, with the exception of suppression experiments, the indicated *CDC24, cdc24, CDC42,* and *cdc42* genes are the sole copies present, and their expression is driven by their endogenous promoters on CEN plasmids. Fusion defects were similar in all strain backgrounds (single and double deletion strains and both mating types).

Plasmids used in this study are listed in Table 2. pRS414CDC24 contains the *CDC24* ORF including 258 base pairs upstream of the ATG and 10 new unique restriction sites in *CDC24* (Nern and Arkowitz, 1998). pRS313CDC24 was constructed by cloning a HindIII/SpeI fragment that contained the *CDC24* ORF into pRS313. pRS414CDC42 and pRS416CDC42 contains the *CDC42* ORF including 521 base pairs upstream of the ATG. Point mutations were generated by site-directed mutagenesis with the Pfu polymerase (Promega, Charbonnieres Les Bains, France) using the DpnI method (Weiner *et al.*, 1994) and identified by the addition or removal of a silent restriction site. For Cdc24-m6p (R416G) an endogenous EcoRV site was removed 1247 base pairs after the ATG, for Cdc42[V36M]p (and all the V36 mutations) a SnaBI site was added 93 base pairs after the ATG, for Cdc42[C18A]p an EarI site was added 53 base pairs after the ATG, and for Cdc42[T35A]p a PstI site was added 102 base pairs after the ATG. All mutations generated were confirmed by sequencing (ABI [Courtaboeuf, France] PRISM big-dye terminator cycle sequencing kit).

For suppression experiments p2μA-TPI-HACDC24, pYes263RGA1, pGRHis-STE20HA, pYesHACDC42, Yep352FUS1/FUS2 (Santos and Snyder, 2003), and Yep352FUS3 (Santos and Snyder, 2003) were used. *CDC24* was cloned into p2μA-TPI (Nern and Arkowitz, 2000b), and subsequently an oligonucleotide encoding a hemagglutinin (HA) epitope was cloned 5′ of the ATG yielding p2μA-TPI-HACDC24. *RGA1* was PCR amplified from genomic DNA using a 5′ primer with a NcoI site preceding the ATG and a 3′ primer with a NotI site after the stop codon, and a NcoI/NotI fragment was cloned into pYes263 (Melcher, 2000). A 3xHA epitope-tagged Ste20p was constructed by PCR-based gene replacement in SEY6210 using p3xHA-His5 (Rayner and Munro, 1998) as template and oligonucleotides with 60 nucleotides 5′ and 3′ of the termination codon. STE20HA was gap repaired from this strain using a pRS424 plasmid containing the *STE20* promoter and *HIS5* gene, resulting in pGRHis-STE20HA. pBSCDC42 was constructed by PCR amplification of *CDC42* from genomic DNA using a 5′ primer with a HindIII site preceding the ATG and a 3′ primer 147 nucleotides 3′ of the stop codon. The HindIII/blunted *CDC42* PCR product was cloned into a HindIII/SmaI-digested pBluescript KS^- II (Stratagene, Amsterdam, Holland). To generate pYesHACDC42, the *CDC42* ORF was amplified by PCR using a 5′ primer with an in-frame HA epitope preceded by a HindIII site and a 3′ primer with a BamHI site after the stop codon using pBSCDC42 as a template and cloned into pYes2 (Invitrogen, Cergy Pontoise, France).

For localization of Cdc42p, pRS413GFPCDC42, which contained a 521-nucleotide *CDC42* promoter followed by GFP fused to *CDC42,* was used. GFP was PCR amplified using a 5′ primer with a HindIII site preceding the ATG and a 3′ primer with an EcoRI site 5′ of the stop codon. This HindIII/EcoRI-digested PCR product was cloned into appropriately digested pBluescript, yielding pBSGFP. Subsequently *CDC42* was PCR amplified using a 5′ primer with an EcoRI site immediately 3′ of the ATG and a 3′ primer with a BamHI site after the stop codon using pBSCDC42 as a template and cloned into EcoRI/BamHI-digested pBSGFP, yielding pBSGFPCDC42. The promoter region of *CDC42* (521 nucleotides 3′ of ATG) was PCR amplified from genomic DNA using 5′ primer with a XbaI site and a 3′ primer with a HindIII site that replaced 6 nucleotides 5′ of the ATG. This XbaI/HindIII-digested *CDC42* promoter fragment together with a HindIII/SacI GFPCDC42 fragment from pBSGFPCDC42 were cloned into pRS413 digested with XbaI/SacI, yielding p413GFPCDC42. pRS424GALGFPCDC42 was constructed by cloning a BamHI/KpnI GFPCDC42 fragment from pBSGFPCDC42 into appropriately digested pRS424GAL. pRS424GAL was constructed by cloning a NgoMIV/SacII *GAL1* fragment from pRS416GAL into appropriately digested pRS424. pRS416GAL was constructed by cloning a NgoMIV/XbaI *GAL1* fragment from pYes into appropriately digested pRS416. For the localization of Fus1GFP, a 5.2-kb NgoMIV/ScaI FUS1GFP fragment from pRS316FUS1GFP (Santos and Snyder, 2003) was cloned into an appropriately digested pRS413 vector. For septin localization pRS316-CDC3-GFP (Caviston *et al.*, 2003) was used.

For in vitro–coupled transcription-translation, the entire *CDC24* ORF (a 2.6-kb BamHI/SalI fragment) from pEG(KT)CDC24 was cloned into a pT7Tag plasmid (Pollock and Treisman, 1990). Furthermore, the entire *CDC42* ORF was amplified by PCR using a 5′ primer preceded by a BamHI site and a 3′ primer with an XbaI site after the stop codon using pBSCDC42 as a template and cloned into pT7Tag plasmid (Pollock and Treisman, 1990). For MBPCdc42p expression, the entire *CDC42* ORF was PCR amplified using a 5′ primer with an EcoRI site immediately 3′ of the ATG and a 3′ primer with a BamHI site after the stop codon with pBSCDC42 as a template and cloned into

Table 1. Yeast strains used in this study

Strain	Genotype[a]	Source
JY426	*MAT***a**, *leu2-3,-112, ura3-52, his4-34, fus1-Δ1, fus2-Δ3*	Cold Spring Harbor Laboratory
JY429	*MATα, trp1Δ1, ura3-52, cyh2, fus1-Δ1, fus2-Δ3*	Cold Spring Harbor Laboratory
SEY6210	*MATα, leu2-3,-112, ura3-52, his3-Δ200, trp1-Δ901, lys2-801, suc2-Δ9*	S. Emr
SEY6211	*MAT***a**, *leu2-3,-112, ura3-52, his3-Δ200, trp1-Δ901, ade2, suc2-Δ9*	S. Emr
RAY399	*MATα/***a**, *leu2-3,-112/leu2-3,-112, ura3-52/ura3-52, his3-Δ200/his3-Δ200, trp1-Δ901/trp1-Δ901, LYS2/lys2-801, ADE2/ade2, suc2-Δ9/suc2-Δ9*	This study[b]
RAY485	RAY399 *CDC42/cdc42-Δ1::LEU2*	This study
RAY513	SEY6210 *cdc42-Δ1::LEU2* with pRS424GALGFPCDC42	This study[c]
RAY563	SEY6210 *sph1-Δ1::HIS3*	Arkowitz and Lowe (1997)
RAY567	SEY6211 *sph1-Δ1::HIS3*	Arkowitz and Lowe (1997)
RAY950	*MAT***a**, *leu2-3,-112, ura3-52, his3-Δ200, trp1-Δ901, lys2-801, ade2, cdc24::LEU2* with pRS416GalHis$_6$CDC24	Nern and Arkowitz (1998)
RAY1042	RAY950 with pRS414CDC24 instead of pRS416GalHis$_6$CDC24	Nern and Arkowitz (1998)
RAY1052	SEY6211 *cdc24-Δ1::LoxP* with pEG(KT)CDC24	Nern and Arkowitz (2000a)
RAY1142	SEY6211 *cdc24::TRP1 cdc24-m1, bud1Δ::LoxP HIS5Sp LoxP*	Nern and Arkowitz (1999)
RAY1487	SEY6211 *cdc24::TRP1 CDC24, URA3::GFPBUD1*	Nern and Arkowitz (2000a)
RAY1556	SEY6210 *cdc42-Δ1::LEU2* with pRS416CDC42	This study[d]
RAY1565	SEY6210 *cdc42-Δ1::LEU2* with pRS416cdc42[V36M, P69T]	This study[d,e]
RAY1635	SEY6210 *cdc42-Δ1::LEU2* with pRS416cdc42[V36M]	This study[d,f]
RAY1638	SEY6210 *cdc42-Δ1::LEU2* with pRS416cdc42[F37I]	This study[d,f]
RAY1640	SEY6210 *cdc42-Δ1::LEU2* with pRS416cdc42[V36A, A41G]	This study[d,f]
RAY1685	RAY950 with pRS414cdc24-m6 instead of pRS416GalHis$_6$CDC24	Barale *et al.* (2004)
RAY1728	SEY6211 *cdc24-Δ1::LoxP, cdc42-Δ1::LEU2* with pRS414CDC24 and pRS416CDC42	This study[g]
RAY1772	SEY6211 *cdc42-Δ2::HIS5Sp* with pRS416CDC42	This study
RAY1793	SEY6211 *cdc24-Δ1::LoxP, cdc42-Δ1::LEU2* with pRS414CDC24 and pRS416cdc42[V36V][i]	This study[h]
RAY1801	SEY6211 *cdc24-Δ1::LoxP, cdc42-Δ1::LEU2* with pRS414cdc24-m6 and pRS416cdc42[V36V][i]	This study[j]
RAY1830	SEY6211 *cdc24-Δ1::LoxP, cdc42-Δ1::LEU2* with pRS414CDC24 and pRS413GFPCDC42	This study[h]
RAY1833	SEY6211 *cdc24-Δ1::LoxP, cdc42-Δ1::LEU2* with pRS414cdc24-m6 and pRS413GFPCDC42	This study
RAY1907	SEY6210 *sph1-Δ1::HIS3, URA3::GFPBUD1*	This study
RAY1912	SEY6210 *cdc42-Δ1::LEU2* with pRS414cdc42[V36V][i]	This study
RAY1914	SEY6210 *cdc42-Δ1::LEU2* with pRS414cdc42[V36M]	This study
RAY1918	SEY6211 *cdc42-Δ2::HIS5Sp* with pRS414cdc42[V36V][i]	This study
RAY1920	SEY6211 *cdc42-Δ2::HIS5Sp* with pRS414cdc42[V36M]	This study
RAY1926	SEY6211 *cdc42-Δ2::HIS5Sp* with pRS416cdc42[V36M]	This study
RAY1951	SEY6211 *cdc24-Δ1::LoxP, cdc42-Δ1::LEU2* with pRS414CDC24 and pRS413GFPcdc42[V36M]	This study
RAY1952	SEY6211 *cdc24-Δ1::LoxP, cdc42-Δ1::LEU2* with pRS414CDC24 and pRS416cdc42[V36M]	This study[k]
DMY13	SEY6210 *cdc42-Δ1::LEU2* with pRS416cdc42[V36W]	This study[d]
DMY14	SEY6210 *cdc42-Δ1::LEU2* with pRS416cdc42[V36C]	This study[d]
DMY15	SEY6210 *cdc42-Δ1::LEU2* with pRS416cdc42[V36F]	This study[d]
DMY16	SEY6210 *cdc42-Δ1::LEU2* with pRS416cdc42[V36L]	This study[d]
DMY17	SEY6210 *cdc42-Δ1::LEU2* with pRS416cdc42[V36I]	This study[d]
DMY18	SEY6210 *cdc42-Δ1::LEU2* with pRS416cdc42[V36A]	This study[d]
DMY19	SEY6210 *cdc42-Δ1::LEU2* with pRS416cdc42[V36T]	This study[d]
DMY20	SEY6210 *cdc42-Δ1::LEU2* with pRS416cdc42[V36Y]	This study[d]
DMY21	SEY6210 *cdc42-Δ1::LEU2* with pRS416cdc42[V36Q]	This study[d]
DMY22	SEY6210 *cdc42-Δ1::LEU2* with pRS416cdc42[V36S]	This study[d]
DMY23	SEY6210 *cdc42-Δ1::LEU2* with pRS416cdc42[V36H]	This study[d]
DMY25	SEY6210 *cdc42-Δ1::LEU2* with pRS416cdc42[V36K]	This study[d]
DMY26	SEY6210 *cdc42-Δ1::LEU2* with pRS416cdc42[V36R]	This study[d]

[a] *HIS5Sp* refers to *HIS5* from *Schizosaccharomyces pombe*.

[b] Constructed by mating SEY6210 and SEY6211.

[c] Plasmid pRS424GALGFPCDC42 was transformed into RAY399 and tetrads were dissected.

[d] Indicated plasmid pRS416CDC42 or cdc42 mutant was transformed into RAY513 and pRS424GALGFPCDC42 was cured.

[e] Isolated in first *cdc42* mutant screen.

[f] Isolated in second *cdc42* mutant screen.

[g] RAY1052 was transformed with pRS414CDC24 and plasmid pEG(KT)CDC24 was cured. This strain was then crossed to RAY1556 followed by sporulation.

[h] Constructed by transformation of RAY1728 with pRS413GFPCDC42 and pRS416CDC42 was cured (RAY1830). Subsequently strain was transformed with indicated pRS416cdc42 plasmid and plasmid pRS413GFPCDC42 was cured.

[i] Cdc42[V36V] was generated by site-directed mutagenesis of Cdc42p replacing Val 36 with Val (in addition to a silent SnaBI site).

[j] Constructed by transformation of RAY1793 with pRS313CDC24 and pRS414CDC24 was cured. Subsequently strain was transformed with pRS414cdc24-m6 plasmid and plasmid pRS313CDC24 was cured.

[k] Constructed by transformation of RAY1793 with pRS413GFPCDC42 and pRS416cdc42[V36V] was cured. Subsequently the strain was transformed with pRS416cdc42[V36M] plasmid and plasmid pRS413GFPCDC42 was cured.

Table 2. Plasmids used in this study

Plasmid	Vector	Insert	Source
pBS KS$^-$ II			Stratagene
pMal-c2			New England Biolabs
pGEX 6P-2			Amersham
pT7Tag			Pollock and Treisman (1990)
p3xHA-His5	pBS	3xHA-*HIS5Sp*	Rayner and Munro (1998)
pRS313	*CEN HIS3*		Sikorski and Hieter (1989)
pRS413	*CEN HIS3*		Sikorski and Hieter (1989)
pRS414	*CEN TRP1*		Sikorski and Hieter (1989)
pRS416	*CEN URA3*		Sikorski and Hieter (1989)
pRS424	2 μm *TRP1*		Christianson *et al.* (1992)
pRS424GAL	2 μm *TRP1*	*GAL1* promoter	This study
p2μA-TPI	2 μm *ADE2*	*TPI1* promoter	Nern and Arkowitz (2000b)
pYes	2 μm *URA3*		Invitrogen
pYes263	2 μm *URA3*		Melcher (2000)
pGRHis	2 μm *TRP1*	*HIS5Sp*	This study
pRS424GALGFPCDC42	pRS424	GFPCDC42	This study
pBSCDC42	pBS	CDC42	This study
pRS416CDC42	pRS416	CDC42	This study
pRS414CDC42	pRS414	CDC42	This study
pRS413GFPCDC42	pRS413	GFPCDC42	This study
pYesHACDC42	pYes	HACDC42	This study
pT7CDC42	pT7Tag	CDC42	This study
pMalCDC42	pMal-c2	CDC42	This study
pRS414CDC24	pRS414	CDC24	Nern and Arkowitz (1998)
pRS313CDC24	pRS313	CDC24	This study
pRS416GalHis$_6$CDC24	pRS416	His$_6$CDC24	Nern and Arkowitz (1998)
pEG(KT)CDC24	pEG(KT)	CDC24	Nern and Arkowitz (1998)
p2μA-TPI-HACDC24	p2μA-TPI	HACDC24	This study
pT7CDC24	pT7Tag	CDC24	This study
pRS406GFPBud1	pRS406	GFPBud1	Nern and Arkowitz (2000a)
pYes263RGA1	pYes263	RGA1	This study
pGRHis-STE20HA	pGRHis	STE20HA	This study
Yep352FUS1/FUS2	Yep352	FUS1/FUS2	Santos and Snyder (2003)
Yep352FUS3	Yep352	FUS3	Santos and Snyder (2003)
pRS316FUS1GFP	pRS316	FUS1GFP	Santos and Snyder (2003)
pRS413FUS1GFP	pRS413	FUS1GFP	This study
pRS316-CDC3-GFP	pRS316	CDC3-GFP	Caviston *et al.* (2003)
pGEX 6P-CRIB	pGEX 6P-2	CRIB$_{STE20}$	This study

EcoRI/BamHI-digested pMal-c2 (New England Biolabs, Saint Quentin en Yvelines, France). For GST-CRIB pulldown experiments, the CRIB domain of Ste20p was amplified by PCR with primers containing unique BglII and NotI sites. This PCR product, which encodes aa 304-346 of Ste20p, was then cloned into a pGEX 6P-2 plasmid (Amersham, Orsay, France). All constructs were verified by dye terminator sequencing (ABI prism).

Isolation of Mating Mutants

For the initial *cdc42* mutant screen, the entire ORF was amplified with Taq polymerase using mutagenic PCR conditions with pBSCDC42 as a template and cloned into HindIII/XbaI-digested pRS416CDC42 as previously described (Nern and Arkowitz, 1998; Barale *et al.*, 2004). This library was transformed into RAY513, and mating mutants were isolated (Nern and Arkowitz, 1998; Barale *et al.*, 2004). The second screen was carried out in which the Switch I region (amino acids 31-41) was mutagenized using oligonucleotide mixtures. An oligonucleotide encompassing this region (GACTATGTTCCAACAGTGTTCGATAACTATGCG) with 15 base pairs on 5′ and 3′ ends was synthesized in which at each base there was a mixture of 91% indicated base and 3% of the three remaining bases. This frequency was chosen to introduce between two and three nucleotide changes per mutant copy. Ten bacterial clones of this library were sequenced, confirming that mutations were randomly located. In the third screen the valine 36 residue in Cdc42p was changed to 15 different amino acids (V36M, V36A, V36L, V36I, V36P, V36S, V36T, V36Y, V36W, V36Q, V36C, V36K, V36R, V36H, V36E) with the Pfu polymerase (Promega) using the DpnI method (Weiner *et al.*, 1994). These mutants were transformed into RAY513, and viability was assessed by growth on glucose-containing media. Spot matings were also carried out with log phase–growing cells on a lawn of enfeebled tester RAY1142 on a YEPD plate incubated 3 h at 30°C before being replica plated.

Sequence Alignment and Structure Modeling

Sequence alignments were carried out using the BLAST algorithm (Altschul *et al.*, 1990). Structural model threading was generated by homology modeling of the *S. cerevisiae* Cdc42p primary sequence using Swiss-Model service based on the transition state human Cdc42 complex for GTP hydrolysis structure pdb file 2NGR (Nassar *et al.*, 1998).

Mating Assays, Pheromone Response Assays, and Phenotypic Analyses

Patch and quantitative mating were carried out as described (Nern and Arkowitz, 1998) with the indicated tester strain. Bud scars and actin cytoskeleton were visualized with formaldehyde-fixed cells as previously described (Nern and Arkowitz, 1998) except that Alexa-488 phalloidin (Molecular Probes, Cergy Pontoise, France) was used for the latter. Pheromone-induced cell cycle arrest (halo assays), induction of a Fus1LacZ reporter, and cell shape changes were assayed as described (Nern and Arkowitz, 1998, 1999). For quantitative cell fusion assays, matings were performed as described (Barale *et al.*, 2004). Mating pairs included both prezygotes and zygotes, where prezygotes were identified as a mating pair in which only one cell was fluorescent and a septum was visible between the cells. The percentage of prezygotes is the number of prezygotes divided by the total number of mating pairs.

Microscopy

Actin cytoskeleton was imaged using a Deltavision deconvolution microscopy system (Applied Precision, Issaquah, WA) on an Olympus IX-70 microscope (Rungis, France) with an NA 1.4 60× objective. Images were deconvolved using softWoRX, and maximum intensity projections of *Z*-stacks were carried out. Cells were examined using a Leica DMR epifluorescence micro-

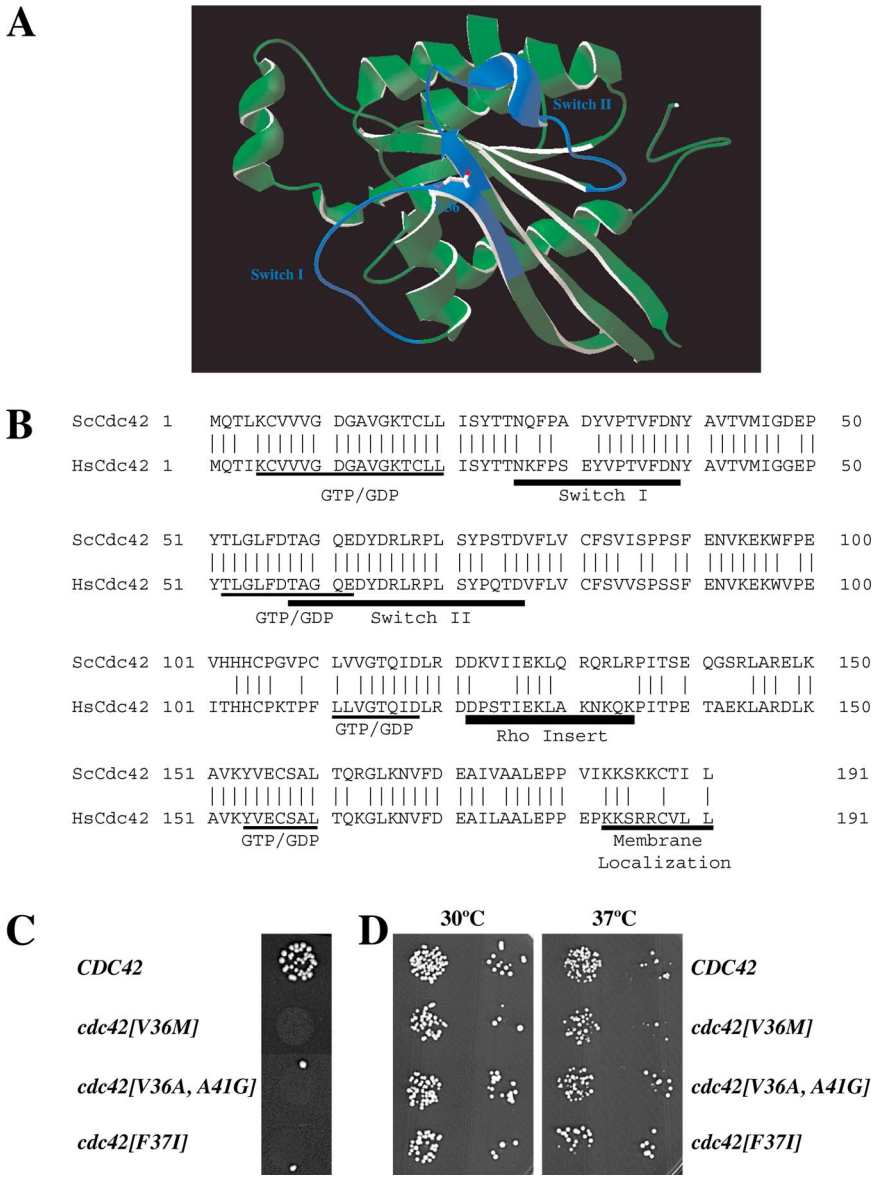

Figure 1. Characterization of *cdc42* mating mutants. (A) Three-dimensional structure model of *S. cerevisiae* Cdc42p. Model generated by homology modeling of *S. cerevisiae* primary sequence using Swiss-Model service based on the transition state Cdc42 complex for GTP hydrolysis structure pdb file 2NGR (Nassar *et al.*, 1998). The amino acid residue Val 36 identified in this study is indicated, and Switch I and Switch II domains are colored in blue. (B) Sequence alignment of *S. cerevisiae* Cdc42p (ScCdc42) and human Cdc42 (HsCdc42). Vertical lines indicate identical residues. Guanine nucleotide-binding domain (GDP/GTP), Switch I and II regions, Rho insert, and membrane localization domain are indicated. (C) Spot mating of *cdc42* mutants isolated from screen of aa 31-41. Matings using strains derived from RAY513 with indicated *CDC42* or *cdc42* gene (as sole copy behind its endogenous promoter on a CEN plasmid) are shown. Matings were carried out with the enfeebled tester RAY1142. (D) *Cdc42* mutants grow normally. Serial dilutions of indicated mutants (same strains as above) were spotted onto YEPD plates and incubated for 2 d at the indicated temperatures.

scope (Rueil-Malmaison, France) with an NA 1.35 100× objective. Images were recorded with a Princeton Instruments Micromax CCD (Roper Scientific, Evry, France), using IPLab (Scanalytics, Rockville, MD) software. Scale bars represent 5 μm.

Immunoblot Analyses

Total yeast protein extracts were prepared (Nern and Arkowitz, 1999) from budding and shmooing cells using 10^7 cells and from mating mixtures using 10^6 cells. Extracts were analyzed by SDS-polyacrylamide gel electrophoresis (PAGE), transferred to nitrocellulose membrane (Amersham), and probed with a polyclonal serum against Cdc42p (1:1000), a mouse monoclonal antibody (mAb) BP1FG (a kind gift from T. Lithgow, 1:10,000) against glyceraldehyde-3-phosphate dehydrogenase, a polyclonal serum against GFP (1:5000; Nern, 2000), or an mAb against HA (HA.11 Babco, Seraing, Belgium, 1:1000). Polyclonal serum against Cdc42p was either from Santa Cruz Biotechnology (Heidelberg, Germany, sc-7172) or from rabbits immunized with MBPCdc42. Immunoblots were visualized by enhanced chemiluminescence (luminol-coumaric acid) on a Fuji-Las3000 (Clichy, France). Equal amounts of cells were used in each experiment, and equal amounts of protein in each lane were confirmed by Ponceau S staining of nitrocellulose membranes.

In Vitro Binding Studies

In vitro–coupled transcription-translation was carried out using a Quick TNT rabbit reticulocyte lysate system (Promega) and 80 μCi [^{35}S]methionine (ICN, Illkirch, France, 1175 Ci/mmol) in a reaction volume of 100 μl using either pT7CDC24, pT7CDC42, pT7cdc42[V36M], or pT7cdc42[T35A], following the manufacturer's instructions.

MBPCdc42 fusion proteins or GSTCRIB fusion protein were expressed in BL21 *Escherichia coli* cells grown at 37°C. After 4-h induction with 0.1 mM IPTG, cells were resuspended in 10% sucrose, 50 mM TrisCl, pH 8, and frozen in liquid nitrogen. All subsequent steps were carried out at 4°C. Cells were lysed by sonication in buffer A (phosphate-buffered saline containing 1 mM EDTA, 1 mM phenylmethylsulfonyl fluoride, 0.1% Triton X-100). Extracts were clarified by centrifugation (10,000 × *g* for 10 min), and fusion proteins were isolated using amylose resin (New England Biolabs) or glutathione Sepharose 4B (Amersham). Protein concentrations were estimated by comparing intensities of bands on Coomassie-stained SDS-PAGE gels.

For Cdc24p Cdc42p bindings amylose resin bound MBPCdc42 was incubated with buffer B (20 mM TrisCl, pH 7.5, 50 mM NaCl, 1 mM DTT, 5% glycerol, 0.1% Triton X-100, and Boehringer Mannheim protease inhibitor, Meylan, France) containing 10 mM EDTA, for 1 h at room temperature in order to strip nucleotides (nucleotide free). To GTPγS load nucleotide free fusion proteins, amylose resin–bound MBPCdc42 was incubated with buffer B containing 10 mM $MgCl_2$ and 120 μM GTPγS (Boehringer Mannheim) for 30 min at room temperature (Hart *et al.*, 1994). For binding assays, MBPCdc42 fusion proteins (~500 ng) bound to amylose resin were incubated with [^{35}S]Cdc24p in 100 μl of buffer B containing either 10 mM EDTA or 10 mM $MgCl_2$ and 120 μM GTPγS for 2 h at 30°C. Amylose resin samples were then washed five times with 100 μl of the respective buffer. Proteins were eluted

with SDS-PAGE sample buffer and analyzed by SDS-PAGE followed by Coomassie blue staining and autoradiography. A Fuji BAS1000 phosphorimager was used for quantification based on two input amounts.

For GSTCRIB pulldown experiments, EDTA (30 μM) was first added to 100 μl of the in vitro–translated [^{35}S]Cdc42p; subsequently GTPγS (0.3 mM) was added, the reaction was incubated at room temperature for 15 min, and finally $MgCl_2$ (200 μM) was added. Subsequently GSTCRIB bound to GSH agarose was added, and reactions were incubated for 1 h at 4°C. Glutathione Sepharose resin samples were then washed five times with 200 μl of GPL buffer (20 mM TrisCl, pH 7.4, 150 mM NaCl, 5 mM $MgCl_2$, 5 mM glycerol phosphate, 1 mM DTT, Boehringer Mannheim protease inhibitor, 0.5% NP-40), and then proteins were eluted in SDS-PAGE sample buffer and analyzed by SDS-PAGE, followed by autoradiography and phosphorimager quantification.

RESULTS

Identification of cdc42 Mating Mutants

To elucidate the functions of the Rho G-protein Cdc42p in the yeast mating process, we screened a randomly mutagenized library for *cdc42* mutants specifically defective in mating, as previously described (Nern and Arkowitz, 1998; Barale *et al.*, 2004). Over 25,000 yeast colonies were tested for mating-specific defects and two mutants were isolated. Sequencing revealed that both mutants had the amino acid alteration V36M. One of these mutants had an additional P69T mutation. Recreation of each individual amino acid change indicated that V36M was responsible for the mating defect. Valine 36 is located in the Switch I region (Figure 1, A and B). Switch I and II regions undergo nucleotide-dependent conformational changes when the two hydrogen bonds between an amino acid from each Switch domain and the gamma phosphate of GTP are released after GTP hydrolysis (Vetter and Wittinghofer, 2001). Structural studies have revealed that these Switch regions show increased flexibility compared with the rest of the G-protein (Farrar *et al.*, 1997; Ito *et al.*, 1997). Hence we mutagenized the region encoding amino acids 31-41 using randomized oligonucleotide mixtures. These oligonucleotide mixtures were designed to introduce on average two to three nucleotide changes in each *CDC42* copy. After screening 3000 yeast transformants, 14 mutants defective in mating were isolated. Sequencing revealed 9 mutants, which had only the V36M amino acid change. Two mutants had the V36M amino acid change in addition to a second change (either D38A or A41R), and two mutants had both the V36A and A41G amino acid alterations. Finally, one mating mutant had a F37I mutation. The *cdc42*[*V36M*], *cdc42*[*V36A, A41G*], and *cdc42*[*F37I*] mutants were all defective for mating when crossed with an enfeebled mating partner (Figure 1C) and did not exhibit any growth defects at 30 and 37°C (Figure 1D).

As the results of these two screens demonstrated that the amino acid residue 36 of Cdc42p is critical for yeast mating, we changed this valine individually to 15 different amino acids in a strain where the mutant *cdc42* was the sole copy (Table 3). Of these 15 different mutants, only the *cdc42*[*V36E*] was inviable. The other mutants could be grouped into three classes based on budding cell morphology and budding pattern: class I cells (L, I, S, Q, and C) exhibited normal morphology, class II cells (A, F, K, and R) were heterogeneous in morphology and in general more elongated, and class III cells (Y and W) were markedly larger than wild-type cells. In addition, three mutants had an intermediate phenotype with *cdc42*[*V36M*] mutant cells somewhat elongated and *cdc42[V36T]* and *cdc42[V36H]* cells both elongated and larger compared with wild-type cells. Mutants in class I budded predominantly with an axial pattern (70–90% axial), class II mutants had a reduced percentage of cells with axial budding (60–70%), and class III mutants budded predominantly with a random pattern (20–50% axial). We examined the ability of the mutants with a normal morphology to mate with an enfeebled tester. Of these mutants (V36I, V36L, V36M, V36S, V36Q, and V36C) only *cdc42[V36M]* was substantially defective in mating. These results indicate that residue 36 in Cdc42p is necessary for both vegetative growth and mating and that the nature of the amino acid residue at this position is critical for these functions. We focused on the *cdc42[V36M]* mutant as it had the strongest mating defect and its vegetative growth was similar to wild-type cells.

Table 3. Morphology, budding pattern, and mating efficiency of *cdc42* mutants

Amino acid 36	Viability	Morphology[a]	Axial bud site selection[b]	Mating efficiency[c]
Val	+	I	89	++
Ala	+	II	65	+
Leu	+	I	nd	++
Ile	+	I	nd	++
Met	+	I/II	75	−
Phe	+	II	nd	nd
Ser	+	I	70	++
Thr	+	II/III	nd	+
Tyr	+	III	nd	++
Trp	+	III	49	−
Gln	+	I	nd	+
Cys	+	I	89	++
Lys	+	II	58	+
Arg	+	II	70	nd
His	+	II/III	22	+
Glu	−	nd	nd	nd

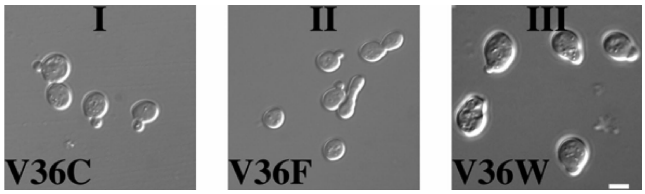

[a] Wild-type morphology (I), elongated cells (II), and large cells (III).
[b] Percentage axial budding pattern (n = 100).
[c] Plate mating efficiency with an enfeebled tester; ++, wild-type efficiency; +, slightly defective; and −, strongly defective.

Cdc42[V36M] Cells Respond to Mating Pheromone by Cell Cycle Arrest, Gene Induction, and Cell Polarization

Several previously isolated *cdc42* mutants were resistant to mating pheromone arrest, including *cdc42[V36A]* (Moskow *et al.*, 2000); hence we examined whether *cdc42[V36M]* cells were able to continue to divide in the presence of α-factor. *MAT**a** CDC42* wild-type and *cdc42[V36M]* mutant cultures were spotted on YEPD plates containing or lacking 8 μg/ml α-factor. Both wild-type and mutant cells were unable to grow in the presence of mating pheromone compared with a control *ste18*Δ mutant that does not respond to pheromone (Whiteway *et al.*, 1989; Figure 2A). Similarly, mating pheromone halo assays were carried out to analyze the pheromone concentration dependence of growth arrest. Figure 2B shows that the growth arrest halos of *CDC42* and *cdc42[V36M]* cells were identical, indicating that this *cdc42* mutant is fundamentally different from the *cdc42[V36A]* mutant previously described. Pheromone-dependent gene induction was examined using a *FUS1-lacZ* reporter and Figure 2C shows that, at saturating α-factor concentration, the

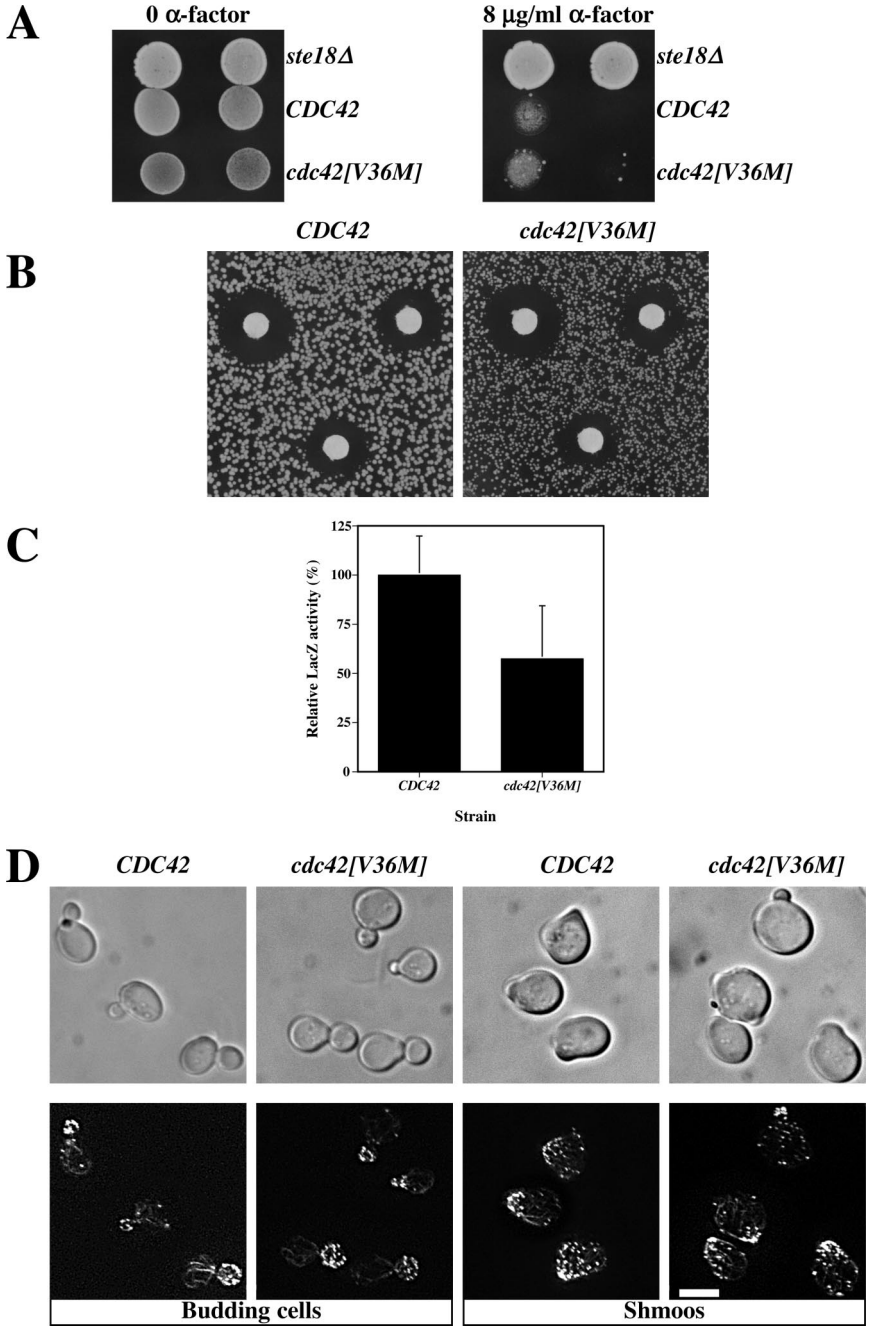

Figure 2. *cdc42[V36M]* cells respond to mating pheromone. (A) *cdc42[V36M]* cells are not resistant to mating pheromone. *CDC42* (RAY1772), *cdc42[V36M]* (RAY1926), and *ste18*Δ strains were spotted on YEPD plates containing or lacking 8 μg/ml α-factor and incubated for 5 d. (B) *cdc42[V36M]* cells arrest growth in the presence of mating pheromone similar to wild-type cells. α-factor (1, 0.5, and 0.2 μg) was spotted on filters placed on a lawn of the indicated strain. Plates were incubated for 3 d. Measurements of the halo diameter indicated ≤5% difference between *CDC42* and *cdc42[V36M]* halos. (C) *cdc42[V36M]* cells induce the mating-specific *FUS1* gene in a pheromone-dependent manner. Cells containing the *FUS1-lacZ* plasmid pSG231 were incubated with 10 μM α-factor for 1 h, and LacZ activity was determined. The means of four determinations from two independent experiments are shown. Error bars, SD. LacZ activity for *CDC42* cells (21.0 Miller units) was set at 100%. (D) *cdc42[V36M]* cells polarize their actin cytoskeleton. DIC and fluorescence images of budding cells and cells treated with 12 μM α-factor for 2 h are shown. Actin cytoskeleton is visualized with Alexa-488 phalloidin. Fluorescence images are maximum intensity projections of *Z*-sections (8–12 × 0.1 μm).

induction level of *FUS1* in *cdc42[V36M]* cells was reduced only twofold compared with *CDC42* cells. The same result was obtained during mating. We next examined the morphology of *cdc42[V36M]* budding cells and shmoos and their actin distribution (Figure 2D). *Cdc42[V36M]* budding cells had a similar morphology compared with a wild-type control; however, the mother cell appeared somewhat rounder in *cdc42[V36M]* mutants (Figures 2D and 5), suggesting that these cells are slightly less polarized than wild-type cells. In response to α-factor, *cdc42[V36M]* cells formed pear-shaped shmoos that were less polarized, with a larger mating projection than wild-type shmoos. Quantitation of the number of cells forming shmoos in the presence of α-factor revealed an identical percentage of shmoos in wild-type and *cdc42[V36M]* strains. Nevertheless, the actin cytoskeleton in wild-type and *cdc42[V36M]* shmoos was similarly polarized. We investigated whether *cdc42[V36M]* cells were able to orient growth toward a pheromone gradient and observed that mating projections of *cdc42[V36M]* cells were not restricted to a location adjacent to the previous bud scar as in chemotropism mutants. Together, these results demonstrate that *cdc42[V36M]* cells respond to mating pheromone.

Cdc42 Mutants Are Defective in Cell Fusion

We next compared the mating efficiency and growth of several *cdc42* mutants: *cdc42[V36M]*, *cdc42[V36A]*, and *cdc42[F37I]* strains isolated in our screen with *cdc42[V36W]* strain (class III morphology) and *cdc42[V36C]* cells (class I morphology). All strains grew at 30°C with *cdc42[V36A]*,

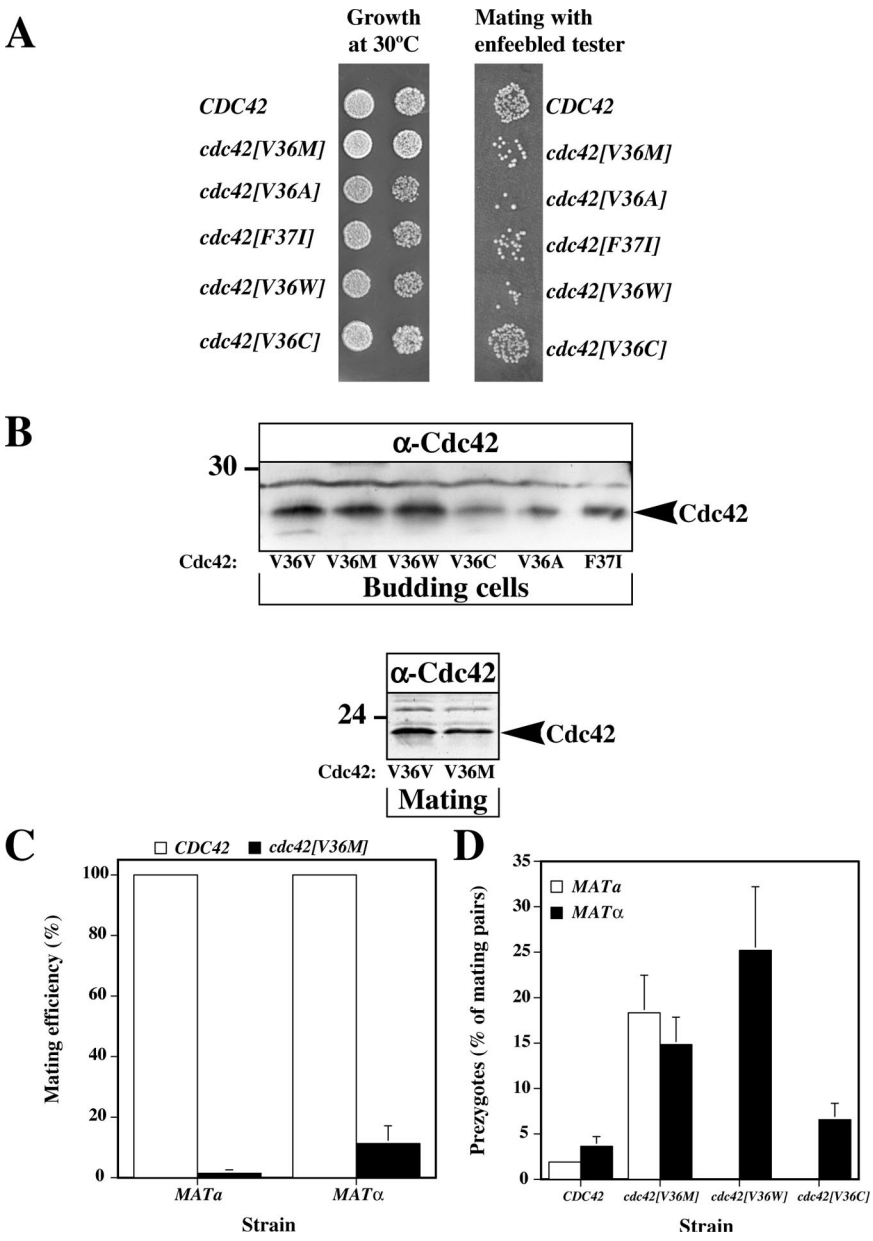

Figure 3. *Cdc42[V36M]* cells have a reduced mating efficiency and accumulate prezygotes. (A) Spot matings and growth of *cdc42* mutants. Serial dilutions of mutants derived from RAY513 with indicated *CDC42* or *cdc42* gene (as sole copy) were spotted onto YEPD plates and incubated for 2 d. Spot matings with indicated strains are shown. Matings were carried out with the enfeebled tester JY426. (B) The expression level of the Cdc42[V36M]p is similar to that of wild type in budding and mating cells. Strains were derived from RAY1772 (*MAT**a***) and RAY513 (*MAT*α) with indicated *CDC42* or *cdc42* gene (as sole copy behind its endogenous promoter on a CEN plasmid). Cell extracts of budding and mating cells were analyzed by SDS-PAGE, followed by immunoblotting and probing with anti-Cdc42p polyclonal sera. Similar results were observed in three independent experiments. (C) The *cdc42[V36M]* mating defect is independent of the mating type. Strains in which *CDC42* or *cdc42[V36M]* is the sole copy behind its endogenous promoter on a CEN plasmid (derived from *MAT**a*** strain RAY1772 or *MAT*α strain RAY513) were used for quantitative matings with a wild-type tester. Values shown are the means of five or six independent experiments with SD indicated and mating efficiencies for *MAT**a*** and *MAT*α *CDC42* strains (1.4 and 3.0%, respectively) set to 100%. (D) *cdc42[V36M]* mating mixtures accumulate prezygotes. Strains with indicated *CDC42* or *cdc42* as sole copy behind its endogenous promoter on a CEN plasmid derived from RAY1772 (*MAT**a***) or RAY513 (*MAT*α) were mated with a GFP-Bud1 expressing strain (RAY1907 or RAY1487). The percentage of prezygotes formed after 4 h was determined as the number of prezygotes (fluorescence in only one cell) divided by the number of mating pairs (prezygotes and zygotes), with values representing the means of 5 to 10 determinations (n = 200–300 mating pairs) from four to eight independent matings. Error bars, SD.

cdc42[F37I], and *cdc42[V36W]* cells forming slightly smaller colonies than wild-type cells. These three mutants together with *cdc42[V36M]* were all defective in mating with an enfeebled tester and formed ~10-20-fold fewer diploid colonies than wild-type and *cdc42[V36C]* cells (Figure 3A). The expression levels of Cdc42p, Cdc42[V36M]p, and Cdc42[V36W]p were similar in budding cells, whereas the expression levels of Cdc42[V36C]p, Cdc42[V36A]p, and Cdc42[F37I]p were reduced (Figure 3B). Furthermore, the expression level of Cdc42[V36M]p in mating cells was similar to that of Cdc42p, indicating that the observed mating defect is not due to an altered expression level. Quantitative matings with an enfeebled mating partner (Figure 3C) demonstrated that the *cdc42[V36M]* mating defect is observed in both mating types, with a 60-fold reduction in mating efficiency in *MAT**a*** cells and a 10-fold reduction in *MAT*α cells. In addition, the *cdc42[V36M]* mutation behaves recessively because its mating defect was complemented by a wild-type copy. We tested whether these mutants were defective in cell fusion, as was previously observed for *cdc24-m6* mating mutant (Barale *et al.*, 2004). The percentage of mating pairs that were prezygotes was quantified after 4-h mating with a wild-type tester whose plasma membrane was labeled with GFP-Bud1. Prezygotes were identified as mating pairs in which GFP fluorescence was observed only in one cell. Figure 3D shows that both mating types of *cdc42[V36M]* cells accumulate prezygotes. In addition, the *cdc42[V36W]*, *cdc42[V36A]*, and *cdc42[F37I]* mutants also accumulate prezygotes during mating but not *cdc42[V36C]* (Figure 3D and unpublished data), indicating that this fusion defect is allele specific. Collectively, these results show that Cdc42p is required for cell fusion during mating, similar to Cdc24p.

Cdc42p Is Required for Localization of Fus1p to the Site of Cell Fusion

We compared the phenotype of *cdc42[V36M]* cells to that of *cdc24-m6* cells. To investigate whether the fusion defect in these two mutants was the result of an inappropriate Cdc42p

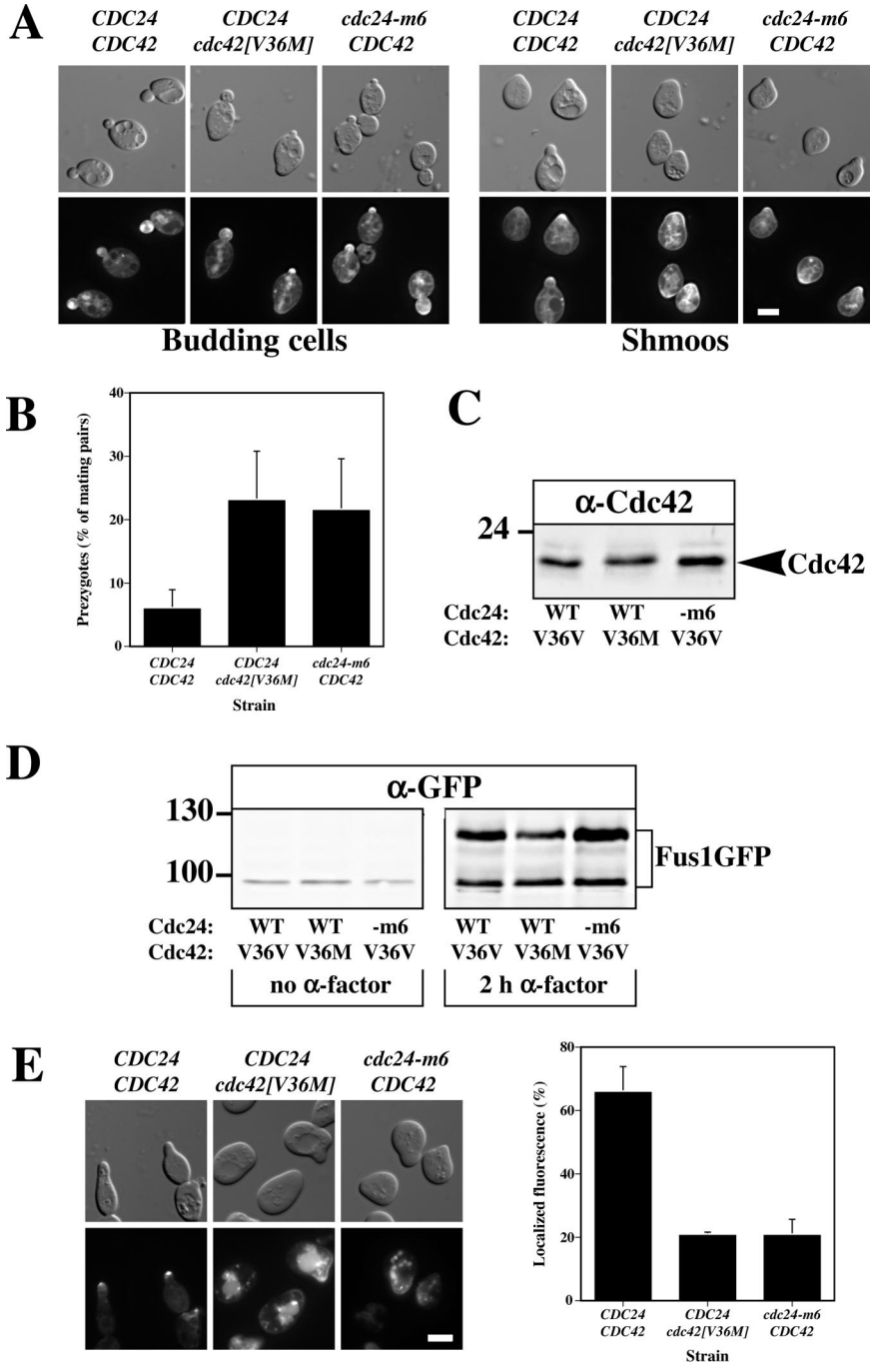

Figure 4. Cdc42p and Cdc24p are required for correct localization of the cell fusion protein Fus1. (A) GFP-Cdc42[V36M] localizes to the bud and shmoo tips. Indicated strains (RAY1830, RAY1951, and RAY1833), which are *MAT**a*** *cdc24*Δ *cdc42*Δ cells carrying a plasmid copy of *CDC24* and GFP-Cdc42 or *CDC24* and GFP-Cdc42[V36M] or *cdc24-m6* and GFP-Cdc42, each behind their respective endogenous promoter on a CEN plasmid, were either grown in the absence (left panels) or presence (right panels) of 12 μM α-factor for 2 h, and fluorescence and DIC images were taken. (B) *cdc24-m6* and *cdc42[V36M]* mating mixtures accumulate similar amounts of prezygotes. Indicated strains (RAY1793, RAY1801, and RAY1952) were mated with RAY1487 (GFP-Bud1) and analyzed as in 3D. Values are the means of four independent matings (n = 200 mating pairs). Error bars, SD. (C) Expression levels of Cdc42p in *CDC42/CDC24*, *cdc42[V36M]/CDC24,* and *CDC42/cdc24-m6* cells. Extracts of logarithmically growing cells (RAY1793, RAY1801, and RAY1952) were analyzed by immunoblot and probed with anti-Cdc42p polyclonal sera. Similar results were observed in three independent experiments. (D) *Cdc42[V36M]* cells induce Fus1-GFP in the presence of mating pheromone. Extracts of cells from the same experiment as above were analyzed by immunoblot either in the absence or presence of α-factor. The lower band is an unglycosylated form of Fus1-GFP. Similar results were observed in three independent experiments. (E) Fus1-GFP is not correctly localized in *cdc24-m6* and *cdc42[V36M]* shmoos. Indicated strains (RAY1793, RAY1801, and RAY1952) carrying a Fus1-GFP plasmid were incubated with 12 μM α-factor for 2 h, and fluorescence images were taken. The mean percentage of shmoos with an observable fluorescence signal at the tip of the mating projection was determined from two independent experiments (n = 200). Bars indicate values.

localization, we determined the localization of a functional GFP-Cdc42 fusion whose expression level was twice that of endogenous Cdc42p. GFP-Cdc42 was expressed in *MAT**a*** *cdc24*Δ *cdc42*Δ cells that carried a plasmid copy of *CDC24* or *cdc24-m6*. GFP-Cdc42[V36M] was expressed in *MAT**a*** *cdc24*Δ *cdc42*Δ cells that carried a plasmid copy of *CDC24,* and this strain exhibited a fusion defect similar to other *cdc42[V36M]* strains. These GFP-Cdc42 and GFP-Cdc42[V36M] fusions localized similarly to the sites of polarized growth (bud and shmoo tips) in wild-type and *cdc24-m6* cells (Figure 4A). Shmoos expressing GFP-Cdc42[V36M] were less polarized than wild-type cells as observed in Figure 2D; however, measurement of the plasma membrane perimeter to which GFP-Cdc42 was enriched revealed that the size of this region was indistinguishable between wild-type and mutant strains (unpublished data). In this isogenic strain *cdc24-m6* and *cdc42[V36M]* mutants accumulate prezygotes to the same extents, consistent with the notion that they have the same molecular defect (Figure 4B). Furthermore, expression levels of Cdc42p and Cdc42[V36M]p were similar in wild-type and mutant cells (Figure 4C). Previously, we demonstrated that Cdc24p was required for localizing the cell fusion protein Fus1p to the site of cell contact and the shmoo tip. In response to α-factor, Fus1-GFP was highly induced in both *cdc24* and *cdc42* mutants despite the approximately twofold

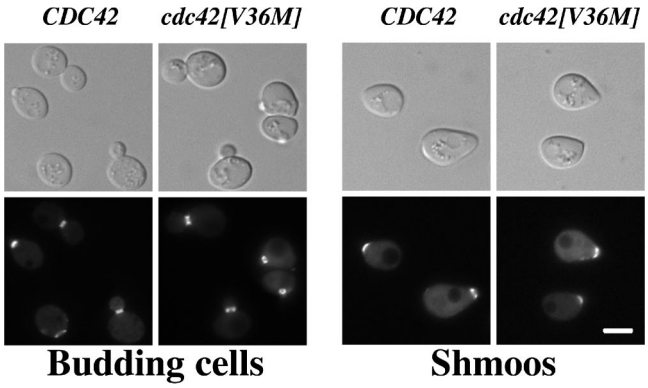

Figure 5. The septin cytoskeleton is unaffected in *cdc42[V36M]* budding and shmooing cells. Indicated strains (RAY1918 and RAY1920) carrying a plasmid copy of Cdc3-GFP behind its endogenous promoter on a CEN plasmid were either grown in the absence (left) or presence (right) of 12 μM α-factor for 2 h, and fluorescence and DIC images were taken.

lower level of Fus1p in *cdc42[V36M]* cells (Figures 2C and 4D). Figure 4E shows that *cdc42[V36M]* and *cdc24-m6* cells are similarly defective in localizing Fus1GFP to the shmoo tip. Overexpression of Fus1p and Fus2p did not suppress the *cdc42[V36M]* fusion defect, indicating that decreased levels of Fus1p are not responsible for this defect. As other *cdc42* mutants in which valine 36 was changed to a threonine, alanine, or glycine had defects in septin organization (Gladfelter *et al.*, 2001, 2002; Caviston *et al.*, 2003), we examined the septin cytoskeleton in wild-type and *cdc42[V36M]* cells growing vegetatively and responding to mating pheromone. Figure 5 shows that the septin cytoskeleton visualized using Cdc3-GFP was identical in wild-type and mutant budding and shmooing cells. The defect in Fus1p localization is therefore not the result of an altered actin or septin cytoskeleton. Thus, two mutants, one in the G-protein Cdc42p and another in its exchange factor Cdc24p, are specifically defective in cell fusion, behave similarly and are both defective in restricting the localization of the cell fusion protein Fus1p to the site of contact.

Cycling of Cdc42p between GDP and GTP States Is Critical for Cell Fusion

One explanation for both the Cdc42p and Cdc24p requirement in cell fusion is that this G-protein needs to be specifically activated by Cdc24p during this process. We first verified that Cdc42[V36M]p was still able to bind Cdc24p in vitro using reticulocyte lysate–translated [^{35}S]Cdc24p and MBPCdc42 or MBPCdc42[V36M] immobilized on amylose resin. Cdc24p binds to both nucleotide free and GTPγS loaded MBPCdc42 and little to no binding was observed with MBP alone (Figure 6, A and B), indicating the binding is specific (Figure 6, A and B). In vitro, Cdc24p binds to a higher extent to Cdc42p•GTPγS compared with the nucleotide free form Cdc42p, similar to results previously observed in vivo (Bose *et al.*, 2001). MBPCdc42[V36M] is able to bind Cdc24p, although to a lower extent than wild-type Cdc42p. This binding was independent of the nucleotide state of Cdc42[V36M]p. If Cdc42[V36M]p was activated to a lower extent than wild-type Cdc42p during mating, we would expect that overexpression of the exchange factor Cdc24p should suppress the fusion defect. Similarly, if Cdc24-m6p was defective in Cdc42p activation, then overexpression of this mutated exchange factor should not affect the fusion defect of *cdc42[V36M]* cells. To address these possibilities, we overexpressed either Cdc24p or Cdc24-m6p

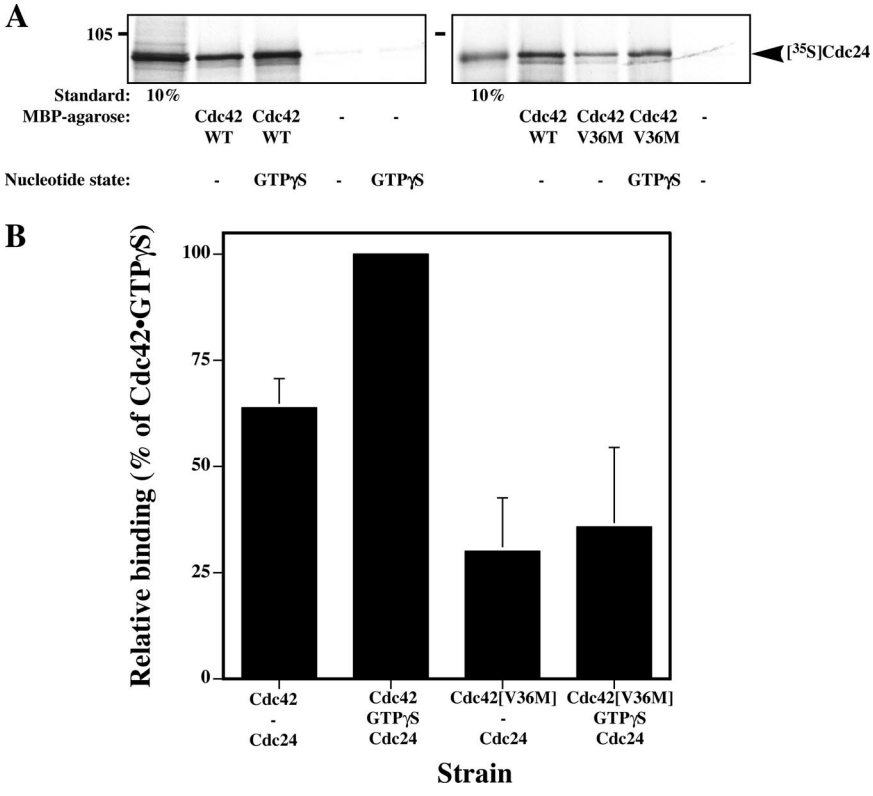

Figure 6. Cdc42[V36M]p can bind Cdc24p in vitro. (A) In vitro–translated [^{35}S]Cdc24p was incubated with resin-immobilized MBP, MBPCdc42, or MBPCdc42[V36M]. Where indicated, MBP fusions were loaded with GTPγS before binding. Binding reactions were analyzed by SDS-PAGE followed by autoradiography. Standard indicates the percentage of [^{35}S]Cdc24p used in the binding reaction. The two different panels are from two independent experiments. (B) Quantitation of Cdc42p–Cdc24p in vitro bindings. A phosphoimager was used for quantitation. Values are the mean of four independent binding experiments. Error bars, SD. Binding of [^{35}S]Cdc24p to Cdc42p•GTPγS (6.8% of input [^{35}S]Cdc24p) was set to 100%.

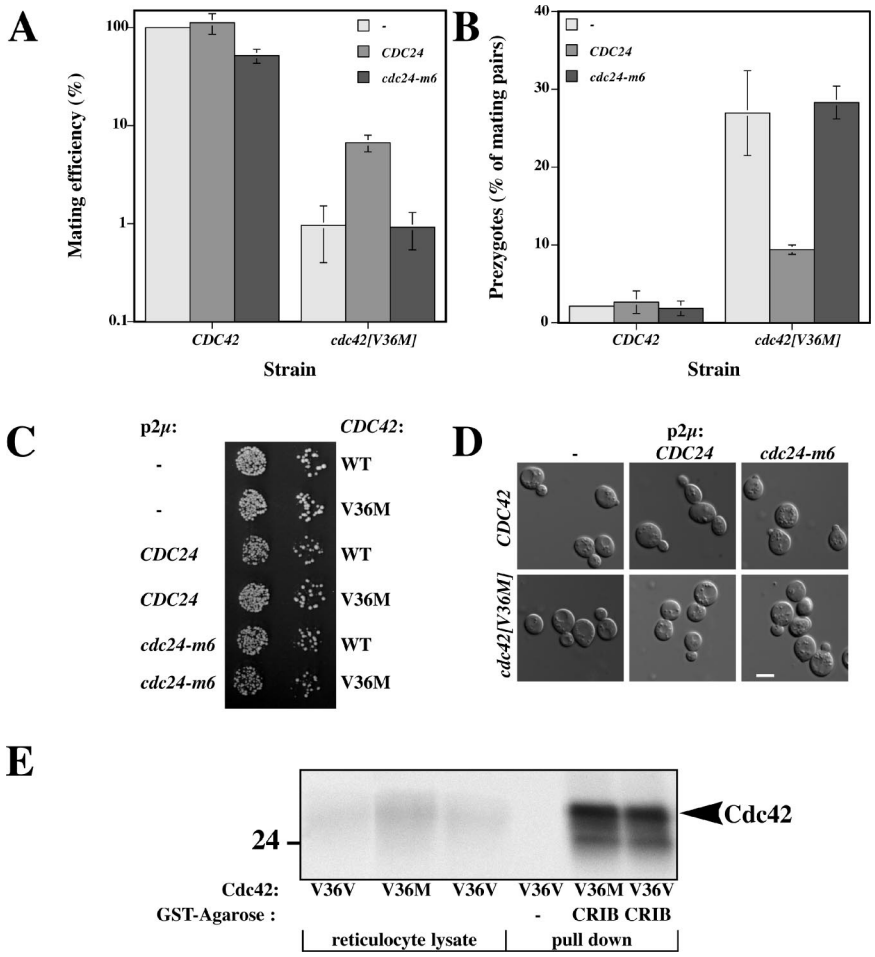

Figure 7. Overexpression of *CDC24* but not *cdc24-m6* partially suppresses fusion defect in *cdc42[V36M]* matings. (A) Overexpression of *CDC24* suppresses mating defect of *cdc42[V36M]* cells. Strains in which *CDC42* or *cdc42[V36M]* is the sole copy behind its endogenous promoter on a CEN plasmid (derived from RAY1918 or RAY1920) and indicated *CDC24* is overexpressed were analyzed for mating efficiency and prezygote formation as described in Figure 3, C and D. Values represent the means of two independent matings, with bars indicating actual values. Matings were carried out with the enfeebled tester JY429. (B) Overexpression of *CDC24* suppresses the fusion defect of *cdc42[V36M]* cells during mating. Values represent the means of two independent matings (n = 200–300 mating pairs), with bars indicating actual values. (C) Overexpression of *CDC24* and *cdc24-m6* does not affect growth of *cdc42[V36M]* cells. Cells were spotted on −Ade plates as described in Figure 3A. (D) Overexpression of *CDC24* or *cdc24-m6* does not affect the morphology of *cdc42[V36M]* cells. DIC images of indicated cells used for above matings grown in −Ade-containing media. (E) Cdc42[V36M]p•GTPγS binds the Ste20p CRIB domain similar to wild-type Cdc42p. [^{35}S]Cdc42p loaded with GTPγS was incubated with GSTCRIB immobilized on amylose resin and bound radioactivity was analyzed by SDS-PAGE followed by autoradiography. Input [^{35}S]Cdc42p reticulocyte lysate (5%) is shown. Quantitation by phosphorimager revealed no difference between Cdc42p and Cdc42[V36M]p GSTCRIB binding, whereas binding of Cdc42[T35A]p was dramatically reduced (unpublished data).

in both *CDC42* and *cdc42[V36M]* cells and examined mating and fusion efficiencies. Overexpression of Cdc24p but not Cdc24-m6p partially suppressed both the mating and fusion defect of *cdc42[V36M]* cells (Figure 7, A and B). Figure 7, C and D, shows that overexpression of Cdc24p and Cdc24-m6p did not affect the growth nor the morphology of wild-type and *cdc42[V36M]* cells, indicating that these levels of exchange factor were not deleterious to the cells. Conversely, overexpression of the Cdc42p GTPase activating protein (GAP), Rga1p, resulted in an increase in the number of prezygotes that accumulate in *cdc42[V36M]* mating mixtures (27% prezygotes accumulated in *cdc42[V36M]* cells carrying an empty vector compared with 40% prezygotes accumulated in *cdc42[V36M]* cells overexpressing Rga1p). These opposing effects of GEF and GAP overexpression are not due to an indirect effect via the MAP kinase cascade as overexpression of the PAK kinase Ste20p and the MAP kinase Fus3p did not alter the percentage of prezygotes that accumulated in *cdc42[V36M]* mating mixtures. Furthermore, Cdc42[V36M]p can still bind the CRIB domain of Ste20p as illustrated by a GSTCRIB pulldown (Figure 7E). Our results rather suggest that the activation or cycling of Cdc42p is critical for efficient cell fusion.

Therefore, we examined if increased levels of wild-type Cdc42p, a GTP-locked Cdc42p mutant (Q61L), or Cdc42p fast cycling mutant such as Cdc42[C18A]p, which has been shown to mimic constitutive activation by the exchange factor (Rossman *et al.*, 2002), could suppress the *cdc24-m6* fusion defect. When Cdc42[Q61L]p was overexpressed, cells grew more slowly and had an abnormal morphology, consistent with previous studies (Ziman *et al.*, 1991). Overexpression of Cdc42[Q61L]p did not markedly affect *cdc24-m6* mating efficiencies (mating efficiency of 8.3 ± 3.2 and 12.8 ± 6.3%, for Cdc42p and Cdc42[Q61L]p overexpression, respectively), nor did it affect the percentage of prezygotes (78 and 75% mating pairs are prezygotes for Cdc42p and Cdc42[Q61L]p overexpression, respectively). These results suggest that an increase in the level of the GTP-bound state is not sufficient for efficient cell fusion, and hence we examined whether overexpression of the fast cycling Cdc42[C18A]p mutant could suppress the fusion defect. As illustrated in Figure 8A, the level of overexpressed Cdc42p and Cdc42[C18A]p were similar in both strains (~20-fold greater than the level of endogenous Cdc42p; unpublished data). Overexpression of Cdc42p did not alter the amount of prezygotes in *cdc24-m6* cells; yet overexpression of Cdc42[C18A]p substantially reduced this amount indicative of a reduction in the fusion defect of *cdc24-m6* matings (Figure 8B). This reduction in cell fusion defect was accompanied by a partial recovery of the *cdc24-m6* mating defect (unpublished data). Budding cells, shmoos, and mating pairs had a similar morphology in all strains (Figure 8C and unpublished data). Interestingly, an increase in Cdc24p levels in *CDC42* cells or Cdc42[C18A]p in *CDC24* cells did not reduce the number of prezygotes, suggesting that in wild-type cells the GDP–GTP cycling is not limiting during the mating. Taken together these results indicate that Cdc42p

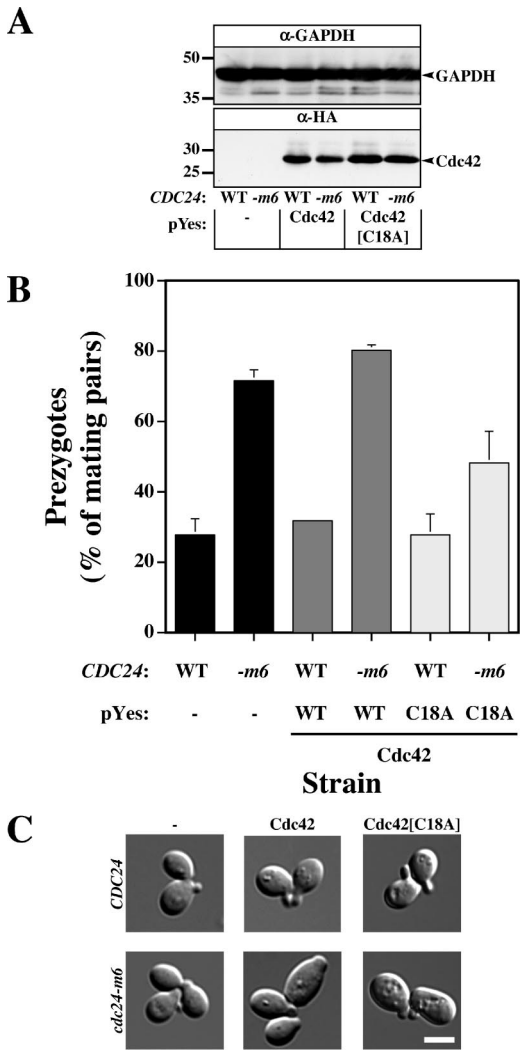

Figure 8. Overexpression of a fast-cycling Cdc42p mutant partially suppresses the *cdc24-m6* cell fusion defect. (A) Expression levels of different Cdc42p versions in *CDC24* and *cdc24-m6* cells. Extracts of logarithmically growing cells (RAY1042, and RAY1685) carrying pYes plasmid with indicated Cdc42p grown in galactose/fructose containing media were analyzed by immunoblot and probed with anti-HA mAb or anti-glyceraldehyde-3-phosphate dehydrogenase (GAPDH) mAb. Similar results were observed in three independent experiments. (B) Overexpression of fast-cycling Cdc42p partially suppresses the *cdc24-m6* cell fusion defect. Cells were grown as described above, mated on galactose/fructose containing media with RAY1487 (GFP-Bud1), and analyzed as in 3D. Values are the means of two independent matings (n = 400 mating pairs). Error bars, SD. (C) Morphology of *CDC24* and *cdc24-m6* budding cells is unaffected by Cdc42p or Cdc42[C18A]p overexpression. DIC Images of indicated cells used for above matings grown in galactose/fructose containing media.

GDP–GTP cycling is important for cell fusion during mating.

DISCUSSION

We have isolated several *cdc42* mutants, which have recessive defects in yeast mating. Our results indicate that the Cdc42p Switch I residue valine 36 is critical for efficient mating. Substitution of this valine by different amino acids indicates that the *cdc42[V36M]* mutant is specifically defective in mating, despite responding to mating pheromone by G_1 arrest, *FUS1* transcription, and shmoo formation. Two-thirds of the viable *cdc42* mutants with valine 36 amino acid substitutions had morphological defects of varying degrees. However, the mating defect of *cdc42[V36M]* cells is not likely to be an indirect result of its weak morphology defect because *cdc42[V36H]*, *cdc42[V36Y]*, and *cdc42[V36K]* mutants with more severe morphological defects all mated with efficiencies similar to the wild-type strain. The *cdc42[V36M]* mutant is defective in cell fusion and accumulates prezygotes during the mating process. This mutant is defective in localizing the component of the fusion machinery, Fus1p to shmoo tip in response to pheromone, similar to the previously isolated *cdc24-m6* mutant. Such a role of Cdc42p in cell fusion is unlikely to be mediated by the MAP kinase cascade because overexpression of Ste20p or Fus3p did not diminish the fusion defect. Furthermore, Cdc42[V36M]p bound the Ste20p CRIB domain identical to wild-type Cdc42p, indicating that this mutant is able to bind CRIB domain–containing effectors. Overexpression of a fast cycling Cdc42p, but not Cdc42p or a GTP-locked mutant, partially suppressed the *cdc24-m6* fusion defect. In addition, overexpression of Cdc24p reduced the fusion defect of *cdc42[V36M]* cells, whereas overexpression of Rga1p enhanced this fusion defect. Together our results strongly suggest that Cdc42p GDP–GTP cycling is necessary for efficient cell fusion during mating, perhaps in activating or localizing the fusion machinery at the site of cell contact.

Roles of Cdc42p in Mating

Different studies have examined the role of the small GTPase Cdc42p and its exchange factor Cdc24p in yeast mating and suggest that these proteins function in different steps of this process. Cdc24p interacts with G$\beta\gamma$ and Far1p, and this complex is required for chemotropic growth toward a mating partner (Valtz *et al.*, 1995; Butty *et al.*, 1998; Nern and Arkowitz, 1998, 1999). More recently, *cdc24* mutants that are defective in cell fusion during mating have been isolated, indicating that this exchange factor functions also in a later step of the mating process (Barale *et al.*, 2004). Cdc42p has been shown to be required for pheromone signaling and Ste20p localization (Moskow *et al.*, 2000). Our work provides evidence for a role of Cdc42p in the cell fusion process. Together, these different analyses of *CDC24* and *CDC42* mutants indicate that this GTPase module is important for chemotropism (*cdc24-m1*), pheromone signaling (*cdc42-md1*), and cell fusion (*cdc24-m6* and *cdc42[V36M]*). The functions of Cdc24p and Cdc42p in these processes are likely to be distinct events as *cdc24-m6* and *cdc42[V36M]* are not defective in pheromone signaling nor chemotropism. Furthermore, Cdc42p interacts with different proteins during pheromone signaling and cell fusion, and these processes are likely to be temporally distinct.

Cdc42p Valine 36 Mutations

Three *cdc42* mutants in which valine 36 is mutated (V36A, V36T, V36G) have been previously characterized. Moskow *et al.* (2000) isolated a *cdc42-md1* in which residues Val36, Lys149, and Leu177 were altered to Ala, Gln, and Ser, respectively. This mutant is pheromone resistant and defective in *FUS1* induction. In a mutant that contained only the Val36Ala substitution, both the pheromone resistance and the gene induction defect were reduced compared with *cdc42-md1*. The Cdc42p[V36A] mutant also had a mild defect in binding the Ste20p CRIB domain, in contrast to

Cdc42p[V36M], which binds the CRIB domain similar to the wild type.

In *cdc42[V36T], cdc42[V36A],* and *cdc42[V36G]* mutants, cells are elongated with wide and misshaped mother bud necks and defects in septin organization, yet the actin cytoskeleton was correctly polarized (Gladfelter *et al.,* 2001, 2002; Caviston *et al.,* 2003). Overexpression of Cla4p suppressed the septin organization defect in *cdc42[V36T]* and *cdc42[V36A]* cells (Gladfelter *et al.,* 2001, 2002). In vitro, Cdc42[V36T]p has reduced intrinsic GTPase activity when compared with wild-type Cdc42p, and overexpression of Rga1p suppressed the septin organization defect in this *cdc42* mutant (Gladfelter *et al.,* 2002). Both Cdc42[V36T]p and Cdc42[V36A]p mutants were shown to be impaired in binding the Cla4p, Ste20p, Gic1p, and Gic2p CRIB domains (Gladfelter *et al.,* 2001).

We consider it unlikely that the cell fusion defect in *cdc42[V36M]* mutants is due to an indirect effect on septin organization for the following reasons. First, both *cdc42[V36T]* and *cdc42[V36A]* cells have a more pronounced morphology defect than *cdc42[V36M]* cells, yet a weaker mating defect. Second, we did not observe any alterations in the septin cytoskeleton in *cdc42[V36M]* cells either during budding or shmooing. Third, overexpression of Rga1p, instead of suppressing the fusion defect in *cdc42[V36M]* cells, increased the fusion defect in this mutant. In summary, our results strongly suggest that the fusion defect in *cdc42[V36M]* cells is not the result of perturbations of the septin cytoskeleton nor pheromone signaling, indicating that alterations in residue 36 in Switch I affect interactions with different effectors, depending on the amino acid substitution.

The Switch I together with the Switch II regions undergo nucleotide-dependent conformational changes. Release of the γ-phosphate upon hydrolysis of GTP allows the Switch regions to relax into the GDP-specific conformation. The Switch I region overlaps with an effector-binding region that includes the adjacent β2 strand and binds, for example, CRIB domain–containing effectors. Targeted molecular dynamics computational techniques have identified the Ras residue equivalent to valine 36 in Cdc42 as a critical hinge in the movements of the Switch I region (Diaz *et al.,* 1997). Replacement of this residue in Ras (Ile 36) with an amino acid with a small side chain, such as glycine, increases the flexibility of this loop and hence accelerates the conformational changes between inactive and active states (Kuppens *et al.,* 1999, 2003). Conversely, it is likely that replacement of valine 36 with either the bulky side chains of methionine or tryptophan residues decreases the flexibility of the Switch I loop and results in the conformational changes between inactive and active states becoming rate limiting in Cdc42, and we speculate that this conformational change is also rate limiting in vivo, in particular during cell fusion. Alternatively, an association of Cdc42[V36M]p with Cdc24p or another protein that stabilizes the interaction with this exchange factor may be reduced in vivo. This affect could be due to alterations in the dynamic properties of the Switch I region as has been suggested for the case of Ras (Spoerner *et al.,* 2004). In either case, overexpression of Cdc24p would be expected to suppress the cell fusion defect as observed.

GDP–GTP Cycling of Cdc42p

Several studies have revealed that Cdc42p GTP hydrolysis is important for the function of this critical G-protein. In budding yeast, using mutants locked in the GTP-bound state (Cdc42[Q61L]p) or deletion of GAPs, it has been suggested that GTP hydrolysis is necessary for septin ring assembly (Gladfelter *et al.,* 2002; Caviston *et al.,* 2003) and establishment of cell polarity (Irazoqui *et al.,* 2003). The inability of this GTP-locked Cdc42p mutant to function in septin ring assembly and cell polarity establishment has led to the suggestion that GDP–GTP cycling is important in these two processes. In mammalian cells a fast cycling version of Cdc42p, which undergoes a rapid GDP–GTP exchange without affecting GTPase activity induces cellular transformation (Lin *et al.,* 1997, 1999). The replacement of alanine for cysteine in the Cdc42[C18A]p fast cycling mutant results in the loss of a hydrogen bond to the nucleotide α-phosphate, a concomitant reduction in GDP affinity and an ~20-fold increase in the GDP–GTP exchange rate in vitro (Rossman *et al.,* 2002). The increased intrinsic exchange rate of this mutant is further enhanced ~10-fold by the presence of the exchange factor Dbs (Rossman *et al.,* 2002). Our results demonstrate that the Cdc42[C18A]p fast cycling mutant can partially suppress the fusion defect of the *cdc24-m6* cells. Neither overexpression of Cdc42p, nor Cdc42[Q61L]p were sufficient to suppress the *cdc24-m6* fusion defect, indicating that the suppression by the fast cycling Cdc42p mutant was specific. Interestingly, overexpression of the Cdc42[C18A]p fast cycling mutant did not affect the fusion efficiency of wild-type cells, suggesting that GDP–GTP cycling is not limiting in this context.

Conversely, it is likely that in *cdc42[V36M]* mutants GDP–GTP exchange is limiting, because overexpression of the exchange factor Cdc24p partially suppresses the fusion defect in these cells. In contrast, overexpression of Cdc24-m6p had no effect on this fusion defect, suggesting that Cdc24-m6p has an altered exchange factor activity, consistent with structure function studies of analogous mutations in the Trio and Tiam1 exchange factors (Liu *et al.,* 1998; Worthylake *et al.,* 2000). It is unlikely that Cdc42[V36M]p GAP interactions are limiting during cell fusion because overexpression of the Rga1p GAP, which functions in yeast mating, did not decrease the fusion defect but rather increased the number of prezygotes that accumulate during mating. Furthermore, two-hybrid interactions between Cdc42[Q61L]p and Rga1p are not affected by the presence of the V36M mutation (S. Barale and R. Arkowitz, unpublished observations), suggesting that Cdc42[V36M]p interacts normally with this GAP. Together, our results strongly suggest that cycling of Cdc42p between GDP and GTP bound forms is important for efficient fusion, perhaps playing a role in correctly localizing and/or activating the fusion machinery.

Cdc42p and Fus1p

Recently, interactions between proteins required for cell fusion and components of the pheromone response pathway and cell polarity proteins were examined in a two-hybrid matrix (Nelson *et al.,* 2004). A number of positive interactions were identified; among them GTP-locked Cdc42p was shown to interact with both Fus1p and Fus2p and Cdc24p with Fus2p (Nelson *et al.,* 2004). These two-hybrid interactions together with the *cdc24* and *cdc42* mutants specifically defective in Fus1p localization that we have isolated suggest that this GTPase module may directly interact with the fusion machinery. We suggest that this specific interaction is necessary for restricting the localization of the fusion machinery, which is required for efficient fusion. We have attempted to coimmunoprecipitate Fus1p using epitope-tagged Cdc42p and conversely Cdc42p using a Fus1GFP fusion in cells treated with α-factor; however, we were unable to detect a stable coimmunoprecipitation (S. Barale and R. Arkowitz, unpublished observations). Hence, although Cdc42p GTP appears to be important for binding Fus1p and Fus2p as measured by two-hybrid assays (Nelson *et al.,*

2004), we favor the notion that Cdc42p GDP–GTP cycling is necessary for assembly and maintenance of the fusion machinery to the site of cell contact and fusion. We propose that assembly of the protein complexes involved in cell fusion requires Cdc42p GTP binding and that GDP–GTP cycling mediated by GEFs and GAPs is critical for cell fusion. The fusion of other cell types as such as myoblast fusion requires the G-protein Rac and the guanine nucleotide exchange factor DOCK180 family member Myoblast city in *Drosophila* (Nolan *et al.*, 1998; Hakeda-Suzuki *et al.*, 2002), suggesting that the regulation of G-protein GDP–GTP cycling is conserved in range of cell fusion processes.

ACKNOWLEDGMENTS

We thank M. Bassilana for constructive criticism, C. Matthews for aid with microscopy, S. Clement for technical assistance, and E. Bi and M. Snyder for plasmids. This work was supported by the Centre National de la Recherche Scientifique, Fondation pour la Recherche Médicale-BNP-Paribas, and La Ligue Contre le Cancer. S.B. was supported by Fellowships from La Ligue Contre le Cancer and Association pour la Recherche sur le Cancer.

REFERENCES

Altschul, S. F., Gish, W., Miller, W., Myers, E. W., and Lipman, D. J. (1990). Basic local alignment search tool. J. Mol. Biol. *215*, 403–410.

Arkowitz, R. A., and Lowe, N. (1997). A small conserved domain in the yeast Spa2p is necessary and sufficient for its polarized localization. J. Cell Biol. *138*, 17–36.

Baba, M., Baba, N., Ohsumi, Y., Kanaya, K., and Osumi, M. (1989). Three-dimensional analysis of morphogenesis induced by mating pheromone alpha factor in *Saccharomyces cerevisiae.* J. Cell Sci. *94*, 207–216.

Barale, S., McCusker, D., and Arkowitz, R. A. (2004). The exchange factor Cdc24 is required for cell fusion during yeast mating. Eukaryot. Cell *3*, 1049–1061.

Bose, I. I., Irazoqui, J. E., Moskow, J. J., Bardes, E. S., Zyla, T. R., and Lew, D. J. (2001). Assembly of scaffold-mediated complexes containing Cdc42p, the exchange factor Cdc24p, and the effector Cla4p required for cell cycle regulated phosphorylation of Cdc24p. J. Biol. Chem. *11*, 7176–7186.

Brizzio, V., Gammie, A. E., Nijbroek, G., Michaelis, S., and Rose, M. D. (1996). Cell fusion during yeast mating requires high levels of a-factor mating pheromone. J. Cell Biol. *135*, 1727–1739.

Brizzio, V., Gammie, A. E., and Rose, M. D. (1998). Rvs161p interacts with Fus2p to promote cell fusion in *Saccharomyces cerevisiae.* J. Cell Biol. *141*, 567–584.

Butty, A. C., Pryciak, P. M., Huang, L. S., Herskowitz, I., and Peter, M. (1998). The role of Far1p in linking the heterotrimeric G protein to polarity establishment proteins during yeast mating. Science *282*, 1511–1516.

Caviston, J. P., Longtine, M., Pringle, J. R., and Bi, E. (2003). The role of Cdc42p GTPase-activating proteins in assembly of the septin ring in yeast. Mol. Biol. Cell *14*, 4051–4066.

Christianson, T. W., Sikorski, R. S., Dante, M., Shero, J. H., and Hieter, P. (1992). Multifunctional yeast high-copy-number shuttle vectors. Gene *110*, 119–122.

Diaz, J. F., Wroblowski, B., Schlitter, J., and Engelborghs, Y. (1997). Calculation of pathways for the conformational transition between the GTP- and GDP-bound states of the Ha-ras-p21 protein: calculations with explicit solvent simulations and comparison with calculations in vacuum. Proteins *28*, 434–451.

Dohlman, H. G., and Thorner, J. W. (2001). Regulation of G protein-initiated signal transduction in yeast: paradigms and principles. Annu. Rev. Biochem. *70*, 703–754.

Dorer, R., Boone, C., Kimbrough, T., Kim, J., and Hartwell, L. H. (1997). Genetic analysis of default mating behavior in *Saccharomyces cerevisiae.* Genetics *146*, 39–55.

Elia, L., and Marsh, L. (1998). A role for a protease in morphogenic responses during yeast cell fusion. J. Cell Biol. *142*, 1473–1485.

Elion, E. A., Trueheart, J., and Fink, G. R. (1995). Fus2 localizes near the site of cell fusion and is required for both cell fusion and nuclear alignment during zygote formation. J. Cell Biol. *130*, 1283–1296.

Farrar, C. T., Halkides, C. J., and Singel, D. J. (1997). The frozen solution structure of p21 ras determined by ESEEM spectroscopy reveals weak coordination of Thr35 to the active site metal ion. Structure *5*, 1055–1066.

Fitch, P. G., Gammie, A. E., Lee, D. J., de Candal, V. B., and Rose, M. D. (2004). Lrg1p Is a Rho1 GTPase-activating protein required for efficient cell fusion in yeast. Genetics *168*, 733–746.

Gammie, A. E., Brizzio, V., and Rose, M. D. (1998). Distinct morphological phenotypes of cell fusion mutants. Mol. Biol. Cell *9*, 1395–1410.

Gladfelter, A. S., Bose, I., Zyla, T. R., Bardes, E. S., and Lew, D. J. (2002). Septin ring assembly involves cycles of GTP loading and hydrolysis by Cdc42p. J. Cell Biol. *156*, 315–326.

Gladfelter, A. S., Moskow, J. J., Zyla, T. R., and Lew, D. J. (2001). Isolation and characterization of effector-loop mutants of *CDC42* in yeast. Mol. Biol. Cell *12*, 1239–1255.

Hakeda-Suzuki, S., Ng, J., Tzu, J., Dietzl, G., Sun, Y., Harms, M., Nardine, T., Luo, L., and Dickson, B. J. (2002). Rac function and regulation during *Drosophila* development. Nature *416*, 438–442.

Hart, M. J., Eva, A., Zangrilli, D., Aaronson, S. A., Evans, T., Cerione, R. A., and Zheng, Y. (1994). Cellular transformation and guanine nucleotide exchange activity are catalyzed by a common domain on the dbl oncogene product. J. Biol. Chem. *269*, 62–65.

Heiman, M. G., and Walter, P. (2000). Prm1p, a pheromone-regulated multispanning membrane protein, facilitates plasma membrane fusion during yeast mating. J. Cell Biol. *151*, 719–730.

Irazoqui, J. E., Gladfelter, A. S., and Lew, D. J. (2003). Scaffold-mediated symmetry breaking by Cdc42p. Nat. Cell Biol. *5*, 1062–1070.

Ito, Y. *et al.* (1997). Regional polysterism in the GTP-bound form of the human c-Ha-Ras protein. Biochemistry *36*, 9109–9119.

Jin, H., Carlile, C., Nolan, S., and Grote, E. (2004). Prm1 prevents contact–dependent lysis of yeast mating pairs. Eukaryot. Cell *3*, 1664–1673.

Johnson, D. I. (1999). Cdc *42*, An essential Rho-type GTPase controlling eukaryotic cell polarity. Microbiol. Mol. Biol. Rev. *63*, 54–105.

Kuppens, S., Diaz, J. F., and Engelborghs, Y. (1999). Characterization of the hinges of the effector loop in the reaction pathway of the activation of ras-proteins. Kinetics of binding of beryllium trifluoride to V29G and I36G mutants of Ha-ras-p21. Protein Sci. *8*, 1860–1866.

Kuppens, S., Hellings, M., Jordens, J., Verheyden, S., and Engelborghs, Y. (2003). Conformational states of the switch I region of Ha-ras-p21 in hinge residue mutants studied by fluorescence lifetime and fluorescence anisotropy measurements. Protein Sci. *12*, 930–938.

Leberer, E., Thomas, D. Y., and Whiteway, M. (1997). Pheromone signalling and polarized morphogenesis in yeast. Curr. Opin. Genet. Dev. *7*, 59–66.

Lin, R., Bagrodia, S., Cerione, R., and Manor, D. (1997). A novel Cdc42Hs mutant induces cellular transformation. Curr. Biol. *7*, 794–797.

Lin, R., Cerione, R. A., and Manor, D. (1999). Specific contributions of the small GTPases Rho, Rac, and Cdc42 to Dbl transformation. J. Biol. Chem. *274*, 23633–23641.

Lipke, P. N., Taylor, A., and Ballou, C. E. (1976). Morphogenic effects of alpha-factor on *Saccharomyces cerevisiae* a cells. J. Bacteriol. *127*, 610–618.

Liu, X. *et al.* (1998). NMR structure and mutagenesis of the N-terminal Dbl homology domain of the nucleotide exchange factor Trio. Cell *95*, 269–277.

Matheos, D., Metodiev, M., Muller, E., Stone, D., and Rose, M. D. (2004). Pheromone-induced polarization is dependent on the Fus3p MAPK acting through the formin Bni1p. J. Cell Biol. *165*, 99–109.

Melcher, K. (2000). A modular set of prokaryotic and eukaryotic expression vectors. Anal. Biochem. *277*, 109–120.

Metodiev, M. V., Matheos, D., Rose, M. D., and Stone, D. E. (2002). Regulation of MAPK function by direct interaction with the mating-specific Galpha in yeast. Science *296*, 1483–1486.

Mosch, H. U., Kohler, T., and Braus, G. H. (2001). Different domains of the essential GTPase Cdc42p required for growth and development of *Saccharomyces cerevisiae.* Mol. Cell. Biol. *21*, 235–248.

Moskow, J. J., Gladfelter, A. S., Lamson, R. E., Pryciak, P.M., and Lew, D. J. (2000). Role of Cdc42p in pheromone-stimulated signal transduction in *Saccharomyces cerevisiae*. Mol. Cell. Biol. *20*, 7559–7571.

Nassar, N., Hoffman, G. R., Manor, D., Clardy, J. C., and Cerione, R. A. (1998). Structures of Cdc42 bound to the active and catalytically compromised forms of Cdc42GAP. Nat. Struct. Biol. *5*, 1047–1052.

Nelson, B., Parsons, A. B., Evangelista, M., Schaefer, K., Kennedy, K., Ritchie, S., Petryshen, T. L., and Boone, C. (2004). Fus1p interacts with components of the Hog1p mitogen-activated protein kinase and Cdc42p morphogenesis

signaling pathways to control cell fusion during yeast mating. Genetics *166*, 66–77.

Nern, A. (2000). The role of the GTP/GDP exchange factor Cdc24p in the control of cell polarity during yeast cell mating. Ph.D. Thesis. Frankfurt am Main: Johann Wolfgang Goethe-Universität.

Nern, A., and Arkowitz, R. A. (1998). A GTP-exchange factor required for cell orientation. Nature *391*, 195–198.

Nern, A., and Arkowitz, R. A. (1999). A Cdc24p, Far1p, G$\beta\gamma$ protein complex required for yeast orientation during mating. J. Cell Biol. *144*, 1187–1202.

Nern, A., and Arkowitz, R. A. (2000a). G proteins mediate changes in cell shape by stabilizing the axis of polarity. Mol. Cell *5*, 853–864.

Nern, A., and Arkowitz, R. A. (2000b). Nucleocytoplasmic shuttling of the Cdc42p exchange factor Cdc24p. J. Cell Biol. *148*, 1115–1122.

Nolan, K. M., Barrett, K., Lu, Y., Hu, K. Q., Vincent, S., and Settleman, J. (1998). Myoblast city, the *Drosophila* homolog of DOCK180/CED-5, is required in a Rac signaling pathway utilized for multiple developmental processes. Genes Dev. *12*, 3337–3342.

Oehlen, L. J., and Cross, F. R. (1998). The role of Cdc42 in signal transduction and mating of the budding yeast *Saccharomyces cerevisiae.* J. Biol. Chem. *273*, 8556–8559.

Philips, J., and Herskowitz, I. (1997). Osmotic balance regulates cell fusion during mating in *Saccharomyces cerevisiae.* J. Cell Biol. *138*, 961–974.

Pollock, R., and Treisman, R. (1990). A sensitive method for the determination of protein-DNA binding specificities. Nucleic Acids Res. *18*, 6197–6204.

Rayner, J. C., and Munro, S. (1998). Identification of the *MNN2* and *MNN5* mannosyltransferases required for forming and extending the mannose branches of the outer chain mannans of *Saccharomyces cerevisiae.* J. Biol. Chem. *273*, 26836–26843.

Read, E. B., Okamura, H. H., and Drubin, D. G. (1992). Actin- and tubulin-dependent functions during *Saccharomyces cerevisiae* mating projection formation. Mol. Biol. Cell *3*, 429–444.

Rose, M. D., Winston, F., and Hieter, P. (1991). Methods in Yeast Genetics: A Laboratory Course Manual, Cold Spring Harbor, NY: Cold Spring Harbor Press.

Rossman, K. L., Worthylake, D. K., Snyder, J. T., Cheng, L., Whitehead, I. P., and Sondek, J. (2002). Functional analysis of cdc42 residues required for Guanine nucleotide exchange. J. Biol. Chem. *277*, 50893–50898.

Santos, B., Duran, A., and Valdivieso, M. H. (1997). CHS5, a gene involved in chitin synthesis and mating in *Saccharomyces cerevisiae.* Mol. Cell. Biol. *17*, 2485–2496.

Santos, B., and Snyder, M. (2003). Specific protein targeting during cell differentiation: polarized localization of Fus1p during mating depends on Chs5p in *Saccharomyces cerevisiae.* Eukaryot. Cell *2*, 821–825.

Sikorski, R. S., and Hieter, P. (1989). A system of shuttle vectors and yeast host strains designed for efficient manipulation of DNA in *Saccharomyces cerevisiae.* Genetics *122*, 19–27.

Simon, M. N., De Virgilio, C., Souza, B., Pringle, J. R., Abo, A., and Reed, S. I. (1995). Role for the Rho-family GTPase Cdc42 in yeast mating-pheromone signal pathway. Nature *376*, 702–705.

Smith, M. G., Swamy, S. R., and Pon, L. A. (2001). The life cycle of actin patches in mating yeast. J. Cell Sci. *114*, 1505–1513.

Spoerner, M., Wittinghofer, A., and Kalbitzer, H. R. (2004). Perturbation of the conformational equilibria in Ras by selective mutations as studied by ^{31}P NMR spectroscopy. FEBS Lett. *578*, 305–310.

Sprague, G.F.J., and Thorner, J. W. (1992). Pheromone response and signal transduction during the mating process of *Saccharomyces cerevisiae.* In: The Molecular and Cellular Biology of the Yeast *Saccharomyces*, Vol. 2, ed. E. W. Jones, J. R. Pringle, and J. R. Broach, Cold Spring Harbor, NY: Cold Spring Harbor Press, 657–744.

Tkacz, J. S., and MacKay, V. L. (1979). Sexual conjugation in yeast. Cell surface changes in response to the action of mating hormones. J. Cell Biol. *80*, 326–333.

Trueheart, J., Boeke, J. D., and Fink, G. R. (1987). Two genes required for cell fusion during yeast conjugation: evidence for a pheromone-induced surface protein. Mol. Cell. Biol. *7*, 2316–2328.

Valtz, N., and Herskowitz, I. (1996). Pea2 protein of yeast is localized to sites of polarized growth and is required for efficient mating and bipolar budding. J. Cell Biol. *135*, 725–739.

Valtz, N., Peter, M., and Herskowitz, I. (1995). FAR1 is required for oriented polarization of yeast cells in response to mating pheromones. J. Cell Biol. *131*, 863–873.

Vetter, I. R., and Wittinghofer, A. (2001). The guanine nucleotide-binding switch in three dimensions. Science *294*, 1299–1304.

Weiner, M. P., Costa, G. L., Schoettlin, W., Cline, J., Mathur, E., and Bauer, J. C. (1994). Site-directed mutagenesis of double-stranded DNA by the polymerase chain reaction. Gene *151*, 119–123.

Whiteway, M., Hougan, L., Dignard, D., Thomas, D. Y., Bell, L., Saari, G. C., Grant, F. J., O'Hara, P., and MacKay, V. L. (1989). The *STE4* and *STE18* genes of yeast encode potential beta and gamma subunits of the mating factor receptor-coupled G protein. Cell *56*, 467–477.

Worthylake, D. K., Rossman, K. L., and Sondek, J. (2000). Crystal structure of Rac1 in complex with the guanine nucleotide exchange region of Tiam1. Nature *408*, 682–688.

Ziman, M., O'Brien, J. M., Ouellette, L. A., Church, W. R., and Johnson, D. I. (1991). Mutational analysis of *CDC42Sc*, a *Saccharomyces cerevisiae* gene that encodes a putative GTP-binding protein involved in the control of cell polarity. Mol. Cell. Biol. *11*, 3537–3544.